International Reviews in Physical Chemistry
Vol. 00, No. 00, Month–Month 2019, 1–56

Applications of ultrafast spectroscopy to sunscreen development, from first principles to complex mixtures

Emily L. Holt[a,b,*] and Vasilios G. Stavros[b,*]

[a]*Molecular Analytical Science Centre for Doctoral Training, Senate House, University of Warwick, Coventry, CV4 7AL, UK*; [b]*Department of Chemistry, University of Warwick, Coventry, CV4 7AL, UK*

(*Received 12 August 2019; Accepted 28 August 2019*)

*Corresponding authors. Email: e.l.holt@warwick.ac.uk; v.stavros@warwick.ac.uk

ISSN: 0144235X print/ISSN 1366591X online

DOI: 10.1080/0144235X.2019.1663062
http://www.tandfonline.com

Sunscreen formulations have been developed to provide an artificial protective barrier against the deleterious effects of overexposure to ultraviolet (UV) radiation in humans. Ultrafast pump-probe spectroscopy techniques have been an invaluable tool in recent years for determining the photochemistry of active ingredients in sunscreen formulations, predominantly UV filters, in both the gas- and solution-phases. These measurements have enabled the elucidation of molecular relaxation pathways and photoprotection mechanisms, which are in turn insightful for assessing a filter's photostability and suitability for sunscreen use. In this review, we discuss the benefits of a *bottom-up* approach: the progression from the study of UV filters for sunscreens in vacuum, away from the influences of any solvent; in solution, to investigate the relaxation pathways of potential sunscreen filters in closer to real-life conditions, whilst exploring the merits of selective functionalisation to improve their characteristics; and beyond, to current advances that are mimicking the application of sunscreen formulations to the surface of the skin.

Keywords: Ultrafast spectroscopy, Sunscreens, Photochemistry, Photostability, Photoprotection

Contents

1. Introduction

Solar radiation consists of a broad spectrum of wavelengths, spanning the infrared (> 700 nm), visible (400 – 700 nm) and ultraviolet (100 – 400 nm) regions of the electromagnetic spectrum. The most topical category within this review is the ultraviolet (UV) region, which is further sub-divided into three groups: the most energetic rays are known as UVC (100 – 290 nm), followed by UVB (290 – 320 nm) and finally UVA (320 – 400 nm) [1]. Overall, UV radiation constitutes approximately 10% of the sun's output prior to its interaction with the Earth's atmosphere [2]. The atmosphere, including the ozone layer, completely blocks UVC and a large proportion of UVB radiation emitted by the sun from reaching the Earth's surface, however the incident UVA radiation remains largely unaffected [3]. Therefore, the radiation that affects life on Earth arises from the UVA and UVB regions of the electromagnetic spectrum [4]. The amount of UV light incident at the Earth's surface can vary, owing to parameters such as vegetation, snow, water, smoke and cloud cover [5–9].

Some benefits of moderated exposure to UVA and UVB radiation have been identified, such as the production of Vitamin D, which can prevent bone conditions such as rickets, osteomalacia and osteoporosis [10, 11]. Evidence also exists that exposure to natural sunlight can improve the symptoms of mental health conditions including seasonal affective disorder and schizophrenia, *via* the production of vitamin D [12, 13]. Other established benefits of moderated sun exposure and its subsequent Vitamin D production include reduced risks of cardiovascular and autoimmune diseases, and improvements in inflammatory skin conditions [14]. These benefits, amongst others, are discussed in the comprehensive reviews by Holick [15] and Hart *et al.* [16]. However, there is a balance to be sought as the adverse effects of overexposure to UV radiation are well-known and characterised, including skin ageing, cataract formation and skin cancer [17–23]. Three main types of skin cancers can arise in patients: basal cell carcinoma, squamous cell carcinoma and malignant melanoma. All three have overexposure to UV radiation attributed as a cause, although in some basal cell carcinoma studies this is debated [24–29]. Malignant melanoma, specifically cutaneous melanoma, is the most aggressive form of skin cancer [30] and has been attributed to 50,000 deaths each year worldwide [31]. Given that current predictions suggest

the incidence of new melanoma cases each year will increase, the number of fatalities should be expected to rise concurrently [32]. There are several potential causes of this upward trend. Firstly, although evidence exists that the ozone layer is now recovering [33, 34], it has previously suffered depletion largely due to human activity, *via* the emission of chlorofluorocarbons (CFCs) and nitrous oxide (N_2O) [35]. Evidence exists that this depletion could have been responsible for observed increases in UVB radiation [36]. Despite the accepted overall improvements in ozone levels, localised depletion still occurs with detrimental consequences. The effects of the unprecedented incidence of ozone depletion in the Arctic during the winters of 2010/11 and 2015/16 propagated throughout the Northern Hemisphere and an increase in UVB levels was detected [34, 37]. Thus, the urgency for efficient UV protection remains, as any increases in carcinogenic UV could further increase the number of skin cancer cases [38]. However, fluctuations in stratospheric ozone are not solely responsible for the rise in melanoma cases [39]. For example, there is growing evidence that UVA radiation, which penetrates the ozone layer, significantly increases levels of skin photodamage and skin cancer risks [22, 40]. This is despite being less carcinogenic and erythrogenic, *i.e.* inducing less redness in the skin, than its higher energy counterparts [40]. Furthermore, tanning the skin remains a popular cosmetic and sociocultural trend, whereby achieving a tan has been cited as a primary motivation for actively seeking UV exposure [14, 41].

1.1. *Challenges in sunscreen development*

Although there are a vast number of sunscreen products available worldwide that could protect us from the adverse effects of UV overexposure, continued research and innovation is still needed in order to overcome the challenges that remain and create the ideal formulation. In the publication by Osterwalder and Herzog [42], four key areas where improvements could be made are identified and summarised, these are: technology, compliance from consumers, measurement/assessment and norms/standards. These sentiments are shared by Burnett *et al.* [43] and both agree that the provision of optimum photoprotection relies upon the convergence of these four criteria.

The overall aim of the technology category is to ensure that there is a versatile repertoire of ingredients for inclusion in sunscreen blends. These blends should reduce the amount of UV radiation reaching the skin over a broad spectral range, with UV filters being central to these efforts [42]. Indeed, the focus of this review is the use of ultrafast spectroscopy methods towards the improvement of UV filters from a photochemical perspective. However, the technology category also incorporates the

sunscreen formulation, which if not correct will result in the active ingredients not being applied uniformly, nor performing to the best of their ability [42, 44].

A sunscreen formulation should also have preferential sensory properties to encourage consumers to apply enough of the product regularly [45]. Ingredients such as silicones and silicas are added to avoid any unpleasant greasy and sticky textures [43, 46]. Moreover, the product should be easy to apply uniformly to ensure homogeneity of the ingredients on the skin. Compliance can only be improved if technologies exist to create aesthetically pleasing formulations that are perceived to offer high levels of sun protection, without any adverse dermatological effects [45]. Examples of such effects include contact dermatitis or allergies following application of the product to the surface of the skin, or photocontact dermatitis, caused by exposure of the product to UV light [47–52]. This ultimate combination remains challenging for sunscreen developers to attain.

As eluded to by Osterwalder and Herzog [42, 44] the assessment of the effectiveness of a sunscreen, *i.e.* how much protection is provided over the entire UVA and UVB range, is crucial. In addition, the standard procedures for measuring efficacy and communicating this to consumers *via* product labelling could also be improved. Together, these measures should also encourage compliance [44].

One of the best-known indicators of sunscreen efficacy is its sun protection factor (SPF), which is a ubiquitous measure of the levels of protection that a sunscreen will provide against sunburn [44]. It is defined by the relation shown in Eq. 1, whose parameters have historically been ascertained *in vivo*, *i.e.* with groups of human volunteers. The abbreviation MED in Eq. 1 stands for minimal erythemal dose: the UV dose (measured in terms of time, or fluence, units $\mathrm{J/m^2}$) needed to induce a minimally detectable redness in the skin, typically 24 hours after irradiation [53, 54]. Erythema is induced mainly by UVB radiation, with UVA wavelengths contributing to a much lower extent [55]. A higher value for the SPF indicates better protection from the wavelengths that induce erythema.

$$\mathrm{SPF} = \frac{\mathrm{MED\ (without\ sunscreen)}}{\mathrm{MED\ (with\ sunscreen)}} \tag{1}$$

Nowadays, defining SPF *via* measurement of MED *in vivo* is not the only method used, owing to its subjective nature and being subject to variability between individuals and laboratories [44, 56, 57]. Furthermore, SPF measurements are expensive, time-consuming, with reproducibility issues and small sample sizes. There are also ethical concerns involved with irradiating volunteers with a known carcinogen [58, 59].

These issues motivate the development of a reliable *in vitro* SPF test; a faster,

cheaper and more ethical alternative to *in vivo* testing, as these tests do not involve human subjects [60]. In this context, *in vitro* testing refers to applying a thin layer (up to 2.5 mg cm^{-2}) of a sunscreen to a synthetic skin substrate and determining the SPF *via* spectrophotometric absorbance and/or transmittance measurements [58, 61]. One form of the equation for *in vitro* SPF determination is shown in Eq. 2 [62, 63]. The term $A(\lambda)$ refers to the value of the erythemal action spectrum at a given wavelength (*i.e.* how much redness is induced by a particular wavelength) [62, 64], $E(\lambda)$ is the solar spectrum irradiance [62, 63, 65] and $T(\lambda)$ is the transmittance of the sample, for the set of wavelengths tested. $A(\lambda)$ and $E(\lambda)$ are constants for any given wavelength.

$$\mathrm{SPF} = \frac{\int_{290}^{400} A(\lambda)E(\lambda)\,\mathrm{d}\lambda}{\int_{290}^{400} A(\lambda)E(\lambda)T(\lambda)\,\mathrm{d}\lambda} \tag{2}$$

Even though the need for *in vitro* SPF testing is apparent, a consensus is yet to be reached on a standardised methodology that suitably correlates with *in vivo* results [54, 58]. Many of the challenges that remain in creating a standardised *in vitro* methodology are issues of reproducibility. Differences between laboratories should be accounted for, both in terms of access to instrumentation and ambient laboratory conditions (*e.g.* temperature, humidity) [60]. In addition, a method is required that will be accurate for all sunscreen samples, which are heterogeneous by nature, with different viscosities and active ingredients. The transmittance properties between any two sunscreen thin layers are a source of variation, even from the same sample. The synthetic skin substrates used for *in vitro* SPF testing are not necessarily identical between tests either, therefore unifying the physical and chemical properties of synthetic skin substrates, as well as the method of applying the test sample to the substrate, remains a key priority [60].

1.1.1. Ideal sunscreen formulation

Contrary to popular belief, SPF alone is not a sufficient measure of sunscreen efficacy. According to the European Commission, sunscreen formulations should satisfy additional performance criteria in addition to a high SPF [46, 66]. A sunscreen should demonstrate: (i) a ratio of UVA protection factor (UVA-PF) to SPF of at least one third [67] and (ii) a critical wavelength of more than 370 nm in order to be marketed as 'broad-spectrum' [42, 68, 69]. The additional criteria, denoted (i) and (ii), ensure close to uniform protection from all UVA and UVB wavelengths, akin to having the skin covered by clothing or avoiding the sun altogether [46, 70]. Standardised ap-

proaches exist to attain the UVA-PF both *in vitro* and *in vivo* to calculate the ratio specified in (i). New sunscreen formulations are thoroughly characterised through the combined use of *in vitro* and *in vivo* approaches [71–73]. A critical wavelength of 370 nm, specified in (ii), means that over 10% of the protection afforded by the sunscreen covers the range 370 – 400 nm.

Indeed, products with a high SPF (≥ 30) do not necessarily satisfy criteria (i) and (ii), as demonstrated in Figure 1. For demonstration purposes in this review, the SPF and UVA protection afforded by three different combinations of UV filters have been calculated *in silico* using a sunscreen simulator [74]. Specific details pertaining to the equations needed for these simulations can be found in the publication by Herzog and Osterwalder [75]. Figure 1 demonstrates the absorbance and transmittance profiles for simulated formulations with different SPFs (50+ and 30, denoted by the black and red lines respectively) that would satisfy the minimum requirements (i) and (ii) outlined above. As a separate comparison, the red and blue lines denote two formulations that would both offer an SPF of 30 and a critical wavelength beyond 370 nm. However, the blue formulation fails to provide the necessary ratio of UVA to UVB protection, despite having marginally higher levels of UVB protection. Figure 1(b) indicates that protection from wavelengths beyond 380 nm requires improvement, as the transmittance of these formulations in this region is high and could invoke skin damage.

1.1.2. Ultraviolet filters

The ingredients that primarily provide UV photoprotection are aptly named UV filters, also known as sunscreen filters. There are two main types of filter: organic (also referred to as chemical filters) and inorganic (physical). The former predominantly absorb UV radiation, whereas the latter can also reflect and scatter radiation [76, 77]. These filters should offer high levels of protection from UV for long periods of time (photostability) [78], without inducing any adverse effects on human health or the environment. Many such undesirable effects of organic UV filters, including endocrine disruption, are documented in the review by Schlumpf *et al.* [79].

With regard to photostability, if a UV filter is not suitably photostable, then exposure to UV light can induce degradation into photoproducts, photofragments or radical species [78]. A high-profile example of such a filter is avobenzone (also known in cosmetics nomenclature as butyl methoxydibenzoylmethane). Use of avobenzone as a UVA filter is widespread globally; in a sunscreen survey conducted by Wang *et al.* [80], 54% of the products from the year 2009 included in their study contained

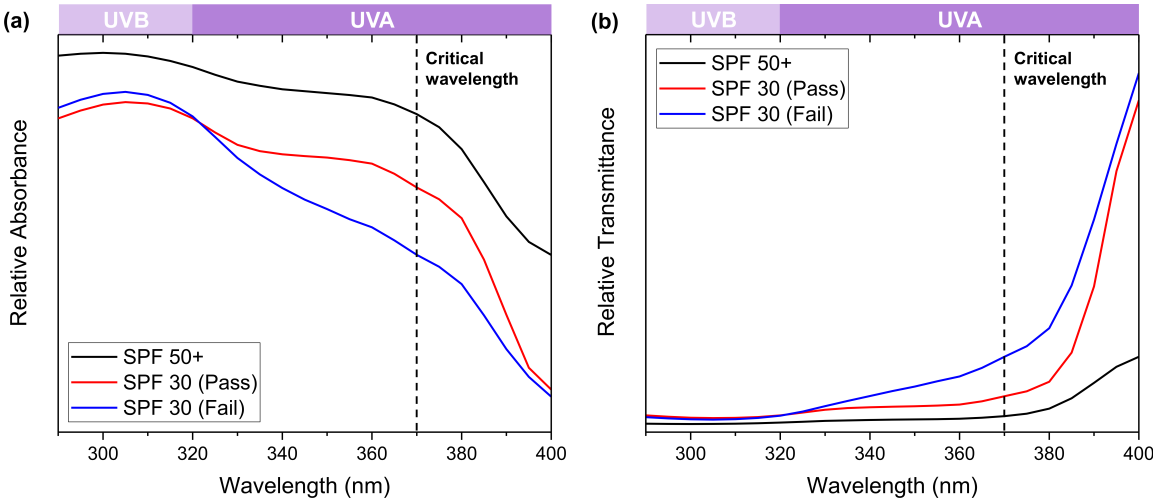

Figure 1. (a) Expected absorbance profiles of sunscreens with SPF 50+ (black line), SPF 30 satisfying UVA protection requirements (red line) and SPF 30 that does not satisfy UVA protection criteria (blue line), as calculated *in silico* using ref. [74]. (b) Corresponding transmission profiles for sunscreens with SPF 50+ (black line), SPF 30 satisfying UVA protection requirements (red line), and SPF 30 sunscreen that does not satisfy these requirements (blue line), calculated *in silico* using ref. [74]. The critical wavelength (370 nm), the wavelength at which more than 10% of the protection should be offered by the formulation, is indicated by the dashed line in both figures. In addition, the regions referred to as UVA (320 – 400 nm) and UVB (290 – 320 nm) are indicated.

avobenzone, up from 16% in 1997. Exposure to UV light can enable avobenzone to undergo *enol-keto* tautomerisation, which is unfavourable given that any depletion in the *enol* species will cause a decrease in the levels of UVA protection afforded by the molecule, as the *keto* form absorbs in the UVC region [81]. This *keto* form of avobenzone is an example of a photoproduct, a light-induced molecular species that differs from the original.

Avobenzone is also known to photofragment: the study by Schwack and Rudolph identifies around a dozen such photoproducts [82]. Two of these, namely the benzil and arylglyoxal photofragments, were later identified by Karlsson *et al.* as cytotoxic and strong skin sensitisers respectively [83]. Due to a lack of alternatives that offer comparable UVA protection, particularly in the United States, sunscreen formulators are restricted to choosing ingredients that will stabilise the *enol* form of avobenzone and prevent all forms of photodegradation.

Several strategies have been developed to prevent the destabilisation of avobenzone within formulations [84]. One approach is to carefully consider which filters should be combined in a formulation for optimum photostability and UV protective coverage. It is known that UV filters can interact with one another with both positive and negative impacts [85, 86]. The photostability of avobenzone has been shown to improve when it is combined with octocrylene, a UVB absorber in its own right, which acts as a triplet quencher [85]. However, not all combinations of avobenzone with UV filters are

favourable; the UVB filter 2-ethylhexyl-4-methoxycinnamate (EHMC) increases the rate of degradation of avobenzone [87] *via* triplet state energy transfer, which in turn induces photolysis and photoisomerisation in the cinnamate [88]. The broadband UV filter bis-ethylhexyloxyphenol methoxyphenyl triazine (also known as bemotrizinol or Tinosorb S) has been shown to stabilise both avobenzone and EHMC, which from a photostability viewpoint makes these filters a viable sunscreen combination [89]. However, Tinosorb S is only approved for sunscreen use in Europe. The variety of approved ingredients in different areas of the world poses additional challenges for sunscreen formulators.

Aside from the problems involved with the use of avobenzone, other UV filters, such as those in the benzophenone and cinnamate families, have been shown to penetrate the skin's surface and induce endocrine disruption [90]. Comprehensive reviews of the endocrine disruption effects of UV filters has been published by Wang *et al.* [91] and Krause *et al.* [92]. In addition, some UV filters commonly found in sunscreens induce detrimental environmental impacts. These impacts include adverse effects to aquatic life, such as: acute and chronic toxicity, effects on reproduction, mutagenicity and bioaccumulation, and coral bleaching [93–98]. As such, reducing the concentrations of these active ingredients is seen as a priority and there are efforts to phase out the most harmful of the existing UV filters. It also remains necessary to increase the repertoire of UV filters that formulators can choose from, particularly for UVA protection where current options are lacking [73]. Therefore, research continues in order to find the next generation of sunscreen filters, which may be more compatible with the surface of human skin, or be more effective at dissipating incident UV energy, whilst posing no risks to the environment. The spectroscopy techniques that will be discussed in this review offer a crucial insight into the mechanism of action of both current and potential UV filters upon photoexcitation, which in turn can contribute to the determination of a filter's effectiveness.

1.2. *Experimental*

In this review, the time-resolved ultrafast spectroscopy techniques that have contributed to the field of sunscreen research thus far will be discussed. The main role of these femtosecond (10^{-15} s) techniques for sunscreen applications has been to elucidate the photoprotection mechanism for individual UV filters in real-time. By understanding how these molecules relax after solar radiation promotes them to an excited state, their potential suitability for sunscreen applications can be assessed. However, these techniques have their limitations: for example, they cannot identify

whether a sunscreen filter is photoallergenic or phototoxic. In this case, complementary biological tests would be needed.

1.2.1. Ultrafast pump-probe spectroscopy

The time-resolved ultrafast spectroscopy techniques discussed in this review fundamentally employ two laser pulses that are femtoseconds in duration, which can, in principle, have central wavelengths ranging from the UV to mid-infrared. The first laser pulse to arrive at the sample is known as the 'pump' pulse, whose role is to photoexcite a small proportion of the molecules in the sample and mimic the action of UVA and UVB radiation upon interaction with UV filters in sunscreen blends. In general, the excitation wavelength is chosen to be its UV-visible absorption maximum (λ_{max}), which for sunscreens usually lies within the UVA or UVB regions and is usually determined by steady-state UV-visible spectroscopy. Following this initial photoexcitation, a corresponding 'probe' pulse then arrives at the sample to give an insight into the evolution of the sample molecules. The time between the pump and probe pulses passing through the sample is known as the 'time delay', where zero is defined to be when the pump and probe arrive at the sample simultaneously. By repeating the pump-probe process and collating transients (snapshots) for a large number of time delays, it is possible to build up a picture of how a molecule decays after photoexcitation, with respect to time. It is worth noting that Strickland and Mourou, the founders of chirped pulse amplification, a necessary step in generating high energy femtosecond laser pulses used in pump-probe techniques, were awarded the 2018 Nobel Prize for Physics [99, 100].

1.2.2. Gas-phase approaches

The first ultrafast gas-phase spectroscopy measurements conducted in the 1980s on the photodissociation of ICN [101] are widely regarded as the 'birth of femtochemistry'. Femtochemistry facilitates the observation and study of fundamental aspects of a chemical reaction in real-time, including bond breaking or formation, and the progression of transition states. It was for this ground-breaking ability to measure such processes using femtosecond spectroscopy that Zewail was awarded the Nobel Prize in Chemistry in 1999 [102–104]. Since then, gas-phase approaches have been utilised to determine intrinsic behaviours of many small molecules in isolation (in the absence of solvent). This information in turn can be used to rationalise molecular behaviour in more realistic environments. The method of taking knowledge garnered in more basic systems/environments and applying that knowledge to more complex systems is known as a *bottom-up* approach. This review will be arranged in accor-

dance with this approach; beginning here with ultrafast time-resolved studies in the gas-phase: time-resolved ion yield (TR-IY), photoelectron spectroscopy (TR-PES) and velocity map imaging (TR-VMI). Detailed reviews of these techniques have been published previously, along with diagrams of instrumental setups [105–110], therefore only a brief description of each experiment is given here.

In many cases, such as in TR-IY experiments, samples are vapourised by heating; this vapour is then seeded into a carrier gas, such as helium or argon. A molecular beam consisting of isolated vibrationally cold molecules, is formed after passing the gaseous mixture into vacuum *via* a nozzle with a small aperture. Suitable nozzle designs for this supersonic jet expansion can be found in the following references [111–115]. The molecular beam is intercepted by the pump and probe pulses at the centre of time-of-flight optics, usually replicating the arrangement described by Wiley and McLaren [116]. The pump photoexcites the sample, then the probe ionises the species, whether that be the excited molecule or any generated photoproducts following photoexcitation. The probe pulse should have sufficient energy to ionise the molecule from its photoexcited (pumped) state, ideally with only a single photon, known as 'soft ionisation'. Soft ionisation techniques ensure that the cation formed has mimimal amounts of internal energy remaining after expulsion of an electron, thus minimising fragmentation. If ionisation (from the excited state) is attained with a single probe photon of equal energy to the pump, this process is known as $1 + 1$ resonance-enhanced multiphoton ionisation ($1 + 1$ REMPI) or resonant two-photon ionisation (R2PI). If the pump and probe photons have different energies, this is denoted $1 + 1'$ REMPI [117–119]. The parent cation (*i.e.* the cation of the sample molecule), as well as any photofragments generated *via* the photoexciting pump pulse (which are subsequently ionised by the probe pulse), are detected using a time-of-flight mass spectrometer. Detection with mass spectrometry ensures that the individual monitoring of parent cations or photofragments is possible, owing to their different mass-to-charge (m/z) ratios. As the time delay (as defined in Section 1.2.1) is varied between the pump and probe pulses, the population of the excited electronic state of the sample molecule, and thus the number of cations produced (the 'ion yield') will often change. By measuring the ion yield signal of the parent cation and photofragments by mass selectivity, the lifetime of this excited electronic state can be determined and decay pathways can be postulated [107, 119].

TR-PES can often be used as a complementary technique to TR-IY for the detection of the free electrons ejected during excited-state photoionisation, as opposed to the ions themselves. The pump and probe pulses for TR-PES experiments serve the same

purpose as TR-IY, to excite and ionise the sample respectively. In this instance, photodetached electrons can be formed with different kinetic energies. These kinetic energies can be identified, for example using a magnetic bottle analyser [108]. The ability to measure the kinetic energies of the photoelectrons in a time-resolved fashion, enables one to track the evolution of the excited state in exquisite detail, as the technique is sensitive to vibrational dynamics and electronic configuration [120, 121]. Lee *et al.* [121] list several processes that have been observed using TR-PES alongside references, including intramolecular vibrational energy redistribution (IVR), internal conversion (IC, as labelled in Figure 2(a)) and intersystem crossing (ISC, Figure 2(a)), amongst other non-adiabatic processes [110, 122–124].

An alternative approach to measuring the kinetic energy of photoelectrons in a time-resolved fashion is to use TR-VMI. In TR-VMI, the photoelectron (or ion) angular distributions are also provided in a single measurement. Charged particle imaging techniques [125] and in particular VMI [126] have revolutionised the fields of photoelectron and photofragment spectroscopies [127–130] and are widely acknowledged methodologies in gas-phase reaction dynamics. Briefly, the collection of charged particles (electrons or ions) being expelled with different kinetic energies form what are known as *Newton spheres* [131]. The three-dimensional (3-D) Newton spheres are converted to a two-dimensional (2-D) image as follows: a position-sensitive detector is placed at the end of a time-of-flight tube; electrons or cations having the same velocities are projected (*via* ion optics) onto the same point of the detector, resulting in the 3-D spheres being flattened to a 2-D image. The detector consists of a set of microchannel plates and a phosphor screen coupled to a charge-coupled device. Following the experiment, the 3-D spheres can be reconstructed from the 2-D image using so-called 'back projection' algorithms [126, 132, 133]. Simultaneous measurement of the kinetic energies and angular distributions of the photoelectrons (or ions), using the position-sensitive detector, enables one to track the evolution of the excited state in unprecedented detail.

In the study by Rodrigues *et al.* [134], TR-PES (utilising a VMI setup) was used to observe vibrational energy redistribution processes in the sunscreen precursor methyl anthranilate (MA, also discussed in Section 2.1) upon photoexcitation with UVA radiation, to conclude that the intramolecular vibrational redistribution in the excited electronic state hinders relaxation to the ground state *via* safe, non-radiative pathways, thus making MA a poor choice for inclusion in a sunscreen. TR-PES has also proven to be a very effective technique to monitor excited state intramolecular proton transfer (ESIPT) [121, 135], a component of the decay mechanism in a multitude of

current UV filters in sunscreens [136]. TR-PES is not focused upon in this review; many excellent reviews discussing TR-PES, its principles and methodologies have been published previously by Stolow and co-workers [108, 124, 137, 138], amongst others [139–141].

Although the gas-phase techniques that will be discussed in this review will focus upon the time domain, specifically femtosecond TR-IY, there are several other laser spectroscopy techniques in the gas-phase that have made invaluable contributions to sunscreen research that it seems appropriate to mention briefly. Firstly, the study by Dean *et al.* [142] on sinapic acid and its derivatives was a pioneering gas-phase study in the frequency domain on plant sunscreens; its significance is highlighted in Section 3.2. The extensive contributions by Ebata and co-workers on the gas-phase photodynamics of cinnamates and sinapates should also be acknowledged [143–148]. Several of these studies [142, 144, 145] and the techniques involved have been reviewed previously by Rodrigues *et al.* [119].

The first combined frequency and time-resolved measurements by Tan *et al.* on the UVB filter 2-ethylhexyl-4-methoxycinnamate (EHMC) [149] have inspired many of the studies discussed in this review; the key results and significance of this study have been detailed previously [150]. In particular, Tan *et al.* [149] demonstrate that frequency- and time-resolved techniques can be a powerful combination for developing knowledge of intrinsic molecular properties, which in turn could be applied within the cosmetics and healthcare industries [150]. Furthermore, the significant impact of microsolvation (in this case generating a cluster of the UV filter with a single water molecule) observed by Tan *et al.* [149] demonstrates the importance of characterising solute-solvent interactions. Such assertions are corroborated in the subsequent combined time and frequency domain study by Kenjo *et al.* [148] on sinapic acid, and the microsolvation study by Domingos and Schnell on oxybenzone (also known as benzophenone-3) [151]. TR-PES on cluster anions could also be a method for offering a molecular-level understanding of condensed phase interactions [140], however this technique has not been extended to sunscreen applications at present.

In addition, gas-phase laser photodissociation spectroscopy has recently been implemented for sunscreen applications for the first time. This first study by Wong *et al.* [152] investigates the potential effects of pH environment on oxybenzone by evaluating different protonation states (both protonated and deprotonated, to represent acidic and alkaline conditions respectively). The motivation arises from sunscreen ingredients becoming exposed to differing pH environments, for example human skin is mildly acidic [153], conversely the water in swimming pools is slightly alkaline

[154]. The authors concluded that the protonation state of oxybenzone, and by consequence pH, has a profound effect on its sunscreening agent properties. There were many differences observed between the photodissociation pathways (and thus the photofragments produced) between the positively and negatively charged species; these fragments were identified by laser-interfaced mass spectrometry. In addition, the absorption properties of the two species were also affected, as identified by gas-phase photodepletion spectra. The study by Wong *et al.* [152] highlights potential future directions for fundamental sunscreen studies. Not only this, the authors also demonstrate the importance of pH studies of UV filters; such studies could inform the development of formulations that are more resilient to the conditions to which they may become exposed.

1.2.3. Solution-phase approaches

This review will predominantly focus upon studies of UV filters in solution, as these ultrafast techniques can be adapted to more closely mimic sunscreen environments that are true-to-life; as such a detailed overview is provided below and the discussion is more extensive throughout.

In the solution-phase, a popular ultrafast technique for studies of sunscreen components is transient (UV-visible) electronic absorption spectroscopy (TEAS). Analogous to the ultrafast gas-phase techniques discussed in Section 1.2.2, the role of the pump pulse for TEAS experiments is to photoexcite a small proportion of the sample molecules. The dynamics of the molecules in the excited state are then probed using a broadband white light pulse (*ca.* 320 – 720 nm). The broad range of wavelengths from the probe pulses facilitate the detection of radiative and non-radiative processes that can occur following photoexcitation. This is in contrast to the gas-phase approaches discussed in Section 1.2.2, when probe pulses are used to ionise the sample molecule. Notably, the sample solution is recirculated after the measurement of each pump-probe pair, to ensure that any degradation products formed are not being probed instead of the molecule of interest [155]. Examples of TEAS experimental setups used for sunscreen research have been published previously [156–159] and a particularly detailed review of the data analysis involved in TEAS has been published by Baker and Stavros [155]. For time-resolved techniques in general, a comprehensive review of global and target data analysis has been published by van Stokkum *et al.* [160].

In addition to TEAS, transient vibrational absorption spectroscopy (TVAS) has also been used for sunscreen applications [161]; the difference between TEAS and

TVAS being that the probe pulse is now in the infrared region, which facilitates the study of excited vibrational modes, rather than electronic states. If bonds are formed and/or broken upon excitation, then these changes can be monitored, as opposed to being speculative on intermediate species formed. The rate of vibrational cooling within molecules can also be determined [162, 163]. It is worthy of note that in the case of TVAS, the pump pulse can also be in the infrared region [164–166], however to the best of our knowledge there have been no studies relevant to sunscreens that have implemented this capability. Steady-state infrared spectroscopy is usually conducted prior to TVAS measurements, to locate the peak (*i.e.* the vibrational mode) that one wishes to probe, where a change in the molecule is expected due to the incoming pump pulse.

For both TEAS and TVAS experiments, transients are attained *via* the measurement of the change in optical density (ΔOD) of the sample, before and after photoexcitation. This measurement technique has been discussed in detail in separate reviews [155, 157], but it is necessary to discuss here for reference in later discussions.

Firstly, a baseline reading is taken of the sample prior to photoexcitation using the probe pulse only. After a time delay (Δt) from when the sample is pumped, the probe pulse will arrive at the sample. The photoexcited sample will absorb different wavelengths of the probe, compared to the baseline. It is this difference between the transmitted intensities of the probe, before and after photoexcitation (denoted I_0 and I_p respectively) that can be used to determine the relaxation mechanism of the molecule of interest. Using I_0 and I_p as the parameters, with the former being a function of wavelength only and the latter being a function of both wavelength and time delay, the definition of ΔOD is shown in Equation 3.

$$\Delta\mathrm{OD}(\lambda, \Delta t) = -\log_{10}\left(\frac{I_\mathrm{p}(\lambda, \Delta t)}{I_0(\lambda)}\right) \tag{3}$$

One advantage of using ΔOD as the measure is that it is an instrument-independent quantity [155], so results between different TEAS and TVAS systems can be directly compared.

1.2.4. Photophysical processes

The spectra attained in transient absorption experiments are a convolution of the sources of changes in optical density. There are four main sources of these changes: two of the processes result in a negative ΔOD signal in accordance with Equation 3, and the other two processes result in a positive signal, as shown in Figure 2(b). These photophysical processes are outlined here to aid with the discussion of results in Section 3. An extended discussion is justified given that there are more studies related

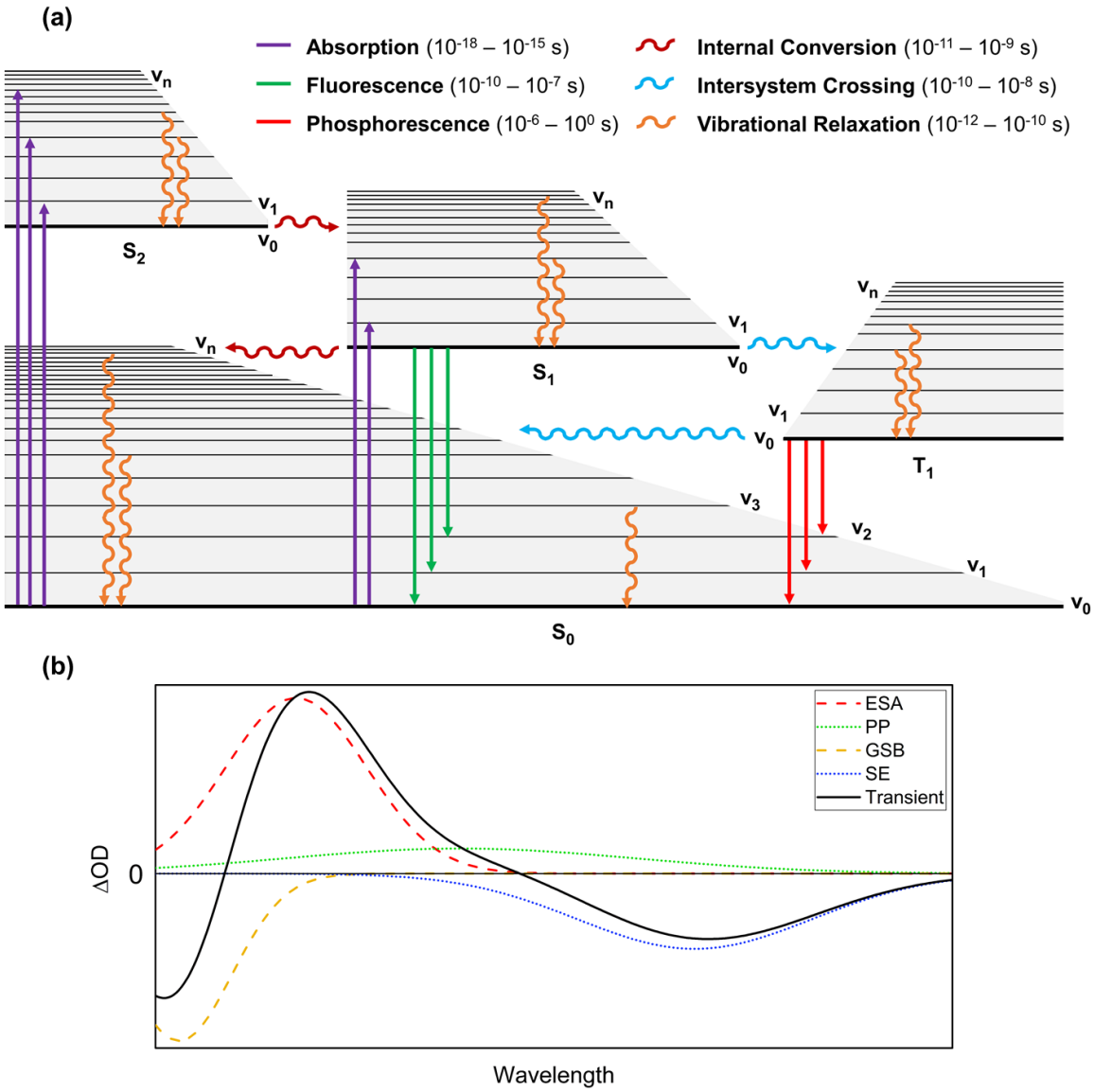

Figure 2. (a) A summary of the main photophysical processes that can occur following photoexcitation (pumping) of a sample in a transient absorption experiment, in the form of a Jablonski diagram. Singlet states are denoted S_i, the lowest energy triplet state is denoted T_1. Vibrational modes are denoted by ν_n. Radiative processes are denoted by the solid lines: absorption in purple, fluorescence in green and phosphorescence in red. Non-radiative processes are denoted by the wavy lines: internal conversion ($S_i \rightarrow S_j$) in dark red, intersystem crossing ($S_i \rightarrow T_j$) in light blue and vibrational relaxation in orange. The timescales for each process [155] are also given. (b) Diagram of possible contributions to a transient absorption spectrum for a given time delay [157]: excited-state absorption (ESA, red dashed line), photoproduct absorption (PP, light green dotted line), ground state bleach (GSB, yellow dashed line), and stimulated emission (SE, blue dotted line). The transient (black solid line) is the sum (convolution) of these contributions.

to sunscreens in solution, perhaps owing to its closer-to-real-life setting, compared to experiments in the gas-phase. Similar outlines of photophysical processes can be found in the publications by Baker and Stavros [155], and Berera *et al.* [157].

The first of the processes that can occur, resulting in a negative signal, is known as a *ground state bleach*. When a fraction of the molecules in the sample are promoted

to the excited electronic state, the number of molecules in the ground electronic state is depleted. Therefore, the absorption from the ground state is now less that in the non-excited sample, creating a so-called 'transparency effect'. Thus, $I_0 < I_p$, which following substitution into Equation 3 gives a negative ΔOD signal. The ground state bleach region often corresponds to the wavelengths of the ground state absorption of the molecule. The second cause of a negative signal is *stimulated emission*. This is caused by a photon from the probe pulse inducing the emission of a second photon from the excited molecule, which subsequently relaxes. Therefore, the amount of light received by the detector will increase, thus $I_0 < I_p$ as before and the signal is negative. Often stimulated emission can be straightforwardly identified as it occurs at similar wavelengths to the fluorescence profile of the molecule, which can be measured using steady-state fluorescence spectroscopy. Stimulated emission is often red-shifted compared to the ground state bleach.

Excited state absorption is the first of the two features that is indicated by a positive ΔOD signal. This feature is due to some wavelengths of the probe being absorbed more in the excited state compared to the ground state. In this case, $I_0 > I_p$ and therefore the signal is positive. The final feature to discuss is the formation of a *photoproduct*. Examples of possible photoproducts are geometric isomers of the original species and photofragments. If these species are formed, they are likely to absorb different regions of the probe pulse compared to the original solvated species. As such, the transmittance of these wavelengths in the pumped sample will decrease, therefore $I_0 > I_p$ as above, and a positive signal is observed. Indications of a photoproduct in ultrafast spectroscopy experiments can often be correlated with the long-term photostability of a molecule, which can be determined using steady-state techniques. For example, UV-visible, Fourier transform infrared (FT-IR) and nuclear magnetic resonance (NMR) spectroscopies can be used to follow the progression of UV irradiation studies [76, 167, 168], which mimic molecular behaviours after long-term exposure to the sun. Steady-state spectroscopy techniques can therefore be considered a strategy to bridge the gap between ultrafast and ultraslow dynamics.

By deducing the contribution of each positive and negative feature to the overall transient absorption spectrum (TAS; note henceforth TAS represents both transient absorption spectrum/spectra), then the spectral features can be assigned to specific photophysical processes, both radiative and non-radiative (as shown in Figure 2(a)).

1.3. *An introductory case study: menthyl anthranilate*

To conclude this introduction, we demonstrate how a *bottom-up* approach to ultrafast spectroscopy can combine with steady-state methods, towards ascertaining the complete relaxation pathway of a UV filter. Thereafter, we show how a filter's potential suitability for sunscreen inclusion can be deduced using these results. As eluded to in Sections 1.1.2 and 1.2, the ideal UV filter should dissipate its energy rapidly (on femtosecond or picosecond timescales), *via* a safe mechanism that is not detrimental to the molecular structure of the filter.

The case study chosen for this demonstration is the UVA sunscreen filter menthyl anthranilate (2-isopropyl-5-methylcyclohexyl 2-aminobenzoate, also known as meradimate, denoted MenA herein). MenA is one of only three organic filters currently approved for use in the United States that provides UVA protection specifically [169]. It is also an approved sunscreen ingredient in Australia [170]. The publication by Rodrigues *et al.* [171] demonstrates how the results from both gas- and solution-phase ultrafast spectroscopy techniques (discussed in Section 1.2) can be combined to gain deeper insights into the photoprotection mechanism of MenA.

Beginning with TR-IY measurements, in line with the *bottom-up* approach, Rodrigues *et al.* [171] identified the presence of a long-lived excited state *in vacuo*. This long-lived state was evidenced by the minimal decrease in parent cation yield within their temporal window and the resulting long decay lifetimes attained ($\gg$ 1.2 ns). TEAS was then used to determine the ultrafast photodynamics of MenA in cyclohexane and methanol, to investigate whether the presence of a solvent bath had any impact upon relaxation. Although subtle differences were observed between the two solvents, suggesting that the molecule's environment may somewhat affect the relaxation mechanism, the dominant feature in both cases was a long-lived species in the excited state [171]. The conclusion was made that, in the case of MenA, the presence of a solvent environment did not alter the overall relaxation pathway. The slow decay was attributed to a long-lived S_1 state that would most likely luminesce regardless of environment [171]. The similarities between the dynamics in the two solvents is perhaps unsurprising, given that a solvatochromic shift in absorbance of only 2 nm was observed for MenA, when measured in 12 different solvent environments of varying polarities [172].

The assignment of luminescence by Rodrigues *et al.* [171] was assisted by a prior steady-state study by Beeby and Jones [173], which confirmed that MenA is highly fluorescent. The measured quantum yield of fluorescence (Φ_f) was 0.64 ± 0.06 in ethanol. Such a high value of Φ_f implies that fluorescence is the dominant relaxation

pathway of MenA. The emission peak was centred around 400 nm, upon excitation at the UVA absorption maximum (340 nm) [173]. Notably, this fluorescence corresponds to the observed stimulated emission feature in the TEAS data by Rodrigues *et al.* [171]. The finding that a large proportion of the fluorescence was emitted in the UVA region ($\leq$ 400 nm) raises the possibility that some of this radiation will be transmitted on to the skin and in fact increase the intensity of the incident radiation at the skin's surface [173]. In addition to fluorescence, a significant proportion of excited MenA molecules underwent $S_1 \rightarrow T_1$ intersystem crossing (ISC) [173]. The ISC quantum yield (Φ_{ISC}) was found to be 0.34 $\pm$ 0.05 in ethanol at room temperature (25°C) by time-resolved thermal lensing techniques [174]. The lifetime of the T_1 state was found to be long-lived ($\sim$ 15 μs), which is an unfavourable trait for a sunscreen as the probability of harmful secondary reactions is increased [174]. For example, triplet states can induce the formation of singlet oxygen species on the skin surface, which can in turn cause extensive DNA damage [175]. The formation of singlet oxygen by MenA was demonstrated in the study by Matsumoto *et al.* [176], which investigated the rate constants of triplet-triplet energy transfer between MenA and typical UVB filters (octocrylene and EHMC) at room temperature. It was determined that the quenching of the T_1 state of MenA with ground state oxygen would indeed produce singlet oxygen. The T_1 state also facilitated triplet-triplet energy transfer to the other UVB filters. Matsumoto *et al.* [176] conclude that the addition of these filters could reduce singlet oxygen generation compared to MenA alone.

By combining all the aforementioned experimental results, the conclusion can be made that MenA does not display the traits of a photophysically ideal sunscreen; it is long-lived, affecting its ability to consistently absorb UVA photons and both the radiative decay pathways (fluorescence and phosphorescence) are potentially harmful. No improvements were seen despite testing in both polar and non-polar solvent systems, therefore it is likely to be challenging to formulate a sunscreen where MenA could act as an ideal UV filter. It is perhaps for these reasons that MenA is now rarely used in sunscreens [177].

To conclude the discussion regarding MenA in this introduction, the potential energy surfaces of the S_0 and S_1 states were calculated computationally. These ascertained the presence of an energy barrier to the conical intersection (CI) between the S_1 charge transfer state and S_0 state, explaining its long-lived nature in the excited state [171]. A full discussion of CIs is outside the scope of this review, however excellent in-depth reviews can be found elsewhere for reference [178–183]. Briefly, a CI is a point of degeneracy between two or more potential energy surfaces of a molecule,

which in the case of MenA facilitates repopulation of the ground state through internal conversion from the S_1 state [159, 171, 184]. The ideal scenario for an efficient sunscreen filter would be to have barrierless access to the CI linking the excited state to the ground state. Throughout this review, the contributions of computational studies to photochemistry studies will be highlighted. In addition, the effects of an inaccessible CI to the photostability of current and potential UV filters will be mentioned in upcoming examples.

2. Gas-phase Spectroscopy Studies

Femtosecond time-resolved gas-phase spectroscopy (discussed in Section 1.2.2) has been used to investigate the dynamics of a multitude of small molecules that undergo many different processes in the excited state. They have proven to be very effective in determining the photodynamics of UV filters *in vacuo*, without the influence of more complex solvent environments. Although it would be almost impossible to provide an exhaustive list of references for the photodynamics of all small molecules studied, the reviews by Stolow *et al.* [108] and Zewail [185] provide excellent starting points.

2.1. *Time-resolved studies: methyl anthranilate*

Methyl anthranilate (MA), a precursor to an approved UVA sunscreen filter in the US (meradimate, also known as menthyl anthranilate, discussed in Section 1.3), has been subject to in-depth study. The study of precursors simplifies the system on a molecular level and facilitates the study of the effect of functional groups on a chromophore. The *ortho* configuration of MA (denoted *o*-MA herein, chemical structure shown in Figure 3(a)) was found not to be an ideal sunscreen candidate *via* the use of gas-phase time-resolved ion yield (TR-IY) [171], as it demonstrated very similar behaviours to MenA (discussed in Section 1.3). Unlike MA and MenA, a sunscreen molecule should, ideally, dissipate its energy on ultrafast timescales (femtoseconds to picoseconds), *via* non-destructive pathways. If this occurs, the molecule can continue to absorb UV photons and afford photoprotection. Minimising the amount of time a molecule spends in its excited state reduces the possibility for a molecule to undergo harmful photochemistry. Comparable molecules to MA and MenA, such as *ortho*-hydroxybenzaldehyde (salicylaldehyde), which possesses a hydroxy group as opposed to a primary amine group in the *ortho* position on the ring, can undergo *enol-keto* tautomerisation within 50 fs. This tautomerisation facilitates subsequent relaxation to the ground electronic state *via* internal conversion [135]. However, in the case of MA, the hydrogen atom involved in the intramolecular hydrogen bond

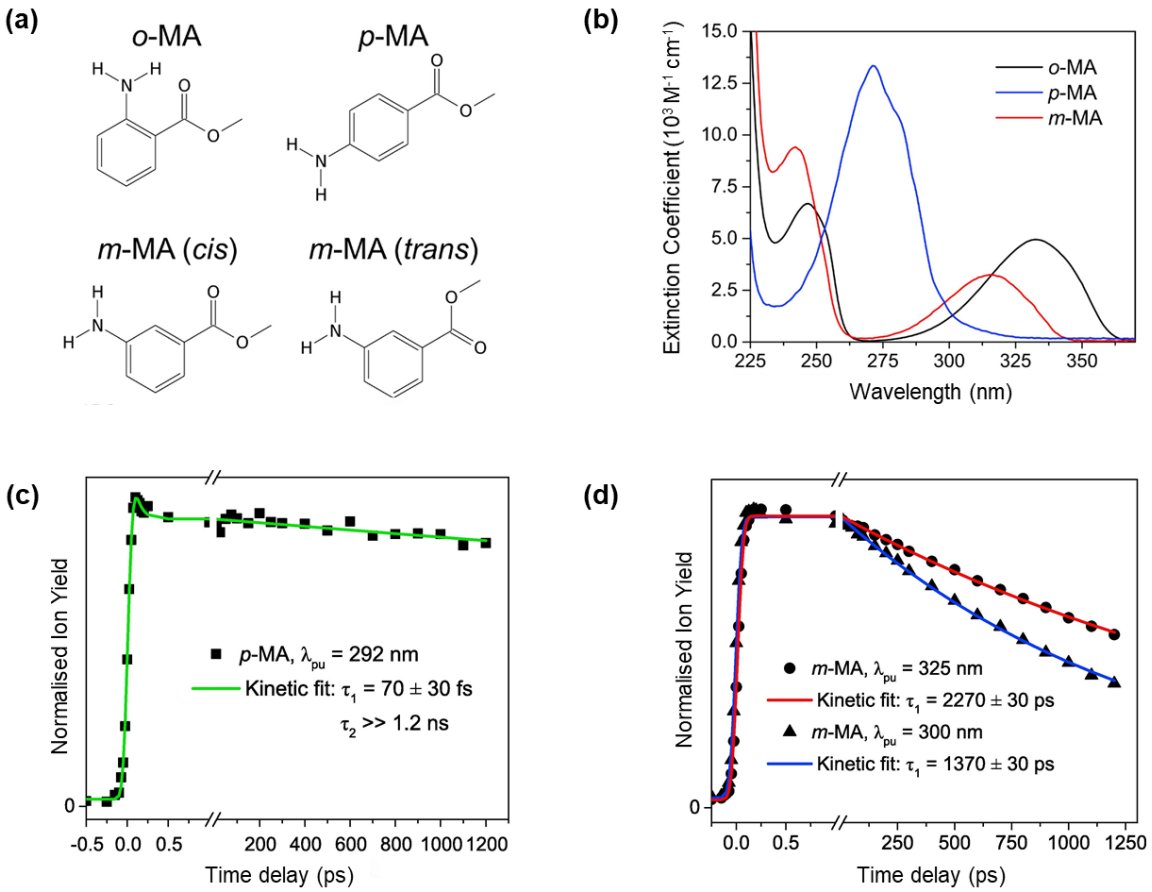

Figure 3. (a): Molecular structures of *o*-MA, *p*-MA and the two rotamers of *m*-MA, (b): UV-visible spectra of o-MA, *p*-MA and *m*-MA taken in the solvent cyclohexane (*o*-MA spectrum first published in ref. [171]). (c) TR-IY transients of *p*-MA, photoexcited at 292 nm (close to the origin of the S_1 state [186]), probed at 315 nm (d) TR-IY transients of two rotamers of *m*-MA, photoexcited at 325 nm (the S_1 origin [187], red trace) and 300 nm (higher energy S_1 excitation, blue trace), probed at 273 nm. Figures reproduced with permission from ref. [188], © Elsevier 2018

between the amino and ester groups, see Fig 3(a), dislocates but does not transfer completely [171]. This traps the excited state energy owing to a barrier to the CI in the S_1 state (discussed in Section 1.3). Following excitation at its peak absorption wavelength ($\lambda_{\text{pump}} = 330$ nm), MA demonstrated a decay lifetime outside the temporal window of the experiment, which was 1.2 ns for the measurements by Rodrigues *et al.* [171]. This remained the case even when the pump wavelength was decreased ($\lambda_{\text{pump}} = 315$ nm). Despite this additional internal energy, it was still insufficient to overcome the energy barrier along the reaction coordinate, en route to the CI. More recently, TR-IY studies have sought to determine whether altering the location of the amino group, and thus removing the intramolecular hydrogen bond formed with the ester group, would improve the photodynamics for use in sunscreens [188]. Gas-phase studies on the effect of substituent position of cinnamic acid derivatives found that *para*-hydroxy cinnamate derivatives were best for sunscreen applications

[189]. In addition, studies on *ortho, meta* and *para*-methoxy methylcinnamates [144] and hydroxy methylcinnamate [146] both showed that changing the position of the methoxy and hydroxy groups respectively had a large influence upon the relaxation dynamics.

In the case of *meta* and *para*-MA, herein referred to as *m*- and *p*-MA (structures shown in Figure 3(a)), TR-IY, alongside complementary steady-state spectroscopy and computational studies revealed that the position of the amino group did indeed impact upon the relaxation dynamics. Firstly, a notable effect of the substituent position on the molecule was observed in the UV-visible spectra of each species when dissolved in cyclohexane, see Figure 3(b), particularly in the case of the *para* species. The *meta* species retains many of the spectral features of the *ortho* species, however the spectrum is spectrally blue-shifted by around 10 nm, thus reducing UVA coverage in this solvent.

Figures 3(c) and (d) show the TR-IY transients recorded for the *meta* and *para* species. The pump pulses (denoted λ_{pu}) photoexcited the S_1 state of each species. For *m*-MA, two λ_{pu} were studied: 325 nm (the S_1 origin [187]) and 300 nm (higher energy S_1 excitation). For *p*-MA, the S_1 and S_2 states were in close proximity [186], and the calculated oscillator strength for the $S_1 \leftarrow S_0$ transition was much lower than $S_2 \leftarrow S_0$ transition. As such, 292 nm was chosen as λ_{pu}, a wavelength close to the S_1 origin that would not induce S_2 excitation.

Just as the UV-visible spectra indicated a discernible impact of substituent position, the TR-IY transients also demonstrate that the position of the amino group has an effect on the decay lifetimes of the S_1 state (as denoted by τ_n in Figure 3, inset in (c) for the *para* species and (d) for the *meta* species). For reference, the TR-IY results for *o*-MA can be found in the earlier publication by Rodrigues *et al.* [171]. The exact values of the decay lifetimes outside of the temporal window of the experiment have to be extrapolated; it is assumed that the decay will continue at the same rate. Rodrigues *et al.* [188] note that the pump pulse will excite both rotamers of *m*-MA (shown in Figure 3(a)). In comparison, the rate of decay for the *para* species is much slower than the *meta* species [188] (ca. Figure 3(c) and 3(d)), and more comparable to the *ortho* species [171]. The long-lived nature of the *para* species was assigned by Rodrigues *et al.* [188] to an inaccessible CI, the existence of which was attained using computational methods [188].

Overall, owing to its faster excited state decay and lower quantum yield of fluorescence than *o*-MA ($25 \pm 5\%$ compared to $> 60\%$ [188, 190]), plus the presence of at least one accessible conical intersection of a prefulvenic nature, *m*-MA is a more

appropriate choice for sunscreen molecular design. Examples of prefulvenic conical intersections, which involve distortion of the benzene ring, have been explored in detail in separate publications [191–194]. Detailed studies on the effect of substituent position on the photodynamics, such as those discussed in this review [144, 146, 188, 189] can be used to inform the design of more efficient sunscreens.

3. Solution-phase Spectroscopy Studies

As detailed in Sections 1.2.2, 1.3 and 2, techniques in the gas-phase offer a critical insight into the photodynamics of sunscreens, as mechanisms can be observed without the complications of intermolecular interactions. That being said, solvating the candidate sunscreen molecules marks the next stage in mimicking a final formulation, *i.e.* the next phase of the *bottom-up* approach. In this section dedicated to solution-phase methods, results from ultrafast transient electronic absorption spectroscopy (TEAS) experiments will be discussed. This technique has been particularly insightful for elucidating potential photoprotection mechanisms upon exposure to UV radiation, as well as determining whether there are any detrimental relaxation pathways.

3.1. *Artificial and Inorganic Sunscreens*

Since the first foray into the ultrafast photodynamics of sunscreens in the solution-phase, a multitude of commercially available UV filters have been investigated using TEAS [195–199]. One of the earliest examples is oxybenzone (OB), a filter that has an absorbance peak in all three UV regions. OB decays on the picosecond timescale when excited at each of its UV-visible absorption maxima (λ_{max}) [161, 200, 201]. The results from these previous studies [161, 200, 201] have been reviewed previously [155]. To summarise, the molecule was initially excited to the S_2 state, confirmed with *ab initio* calculations by Karsili *et al.* [202], with barrierless internal conversion to the S_1 state *via* a CI. Once in the S_1 state, the molecule undergoes ultrafast ($\sim$100 fs) intramolecular hydrogen transfer to form a *keto* isomer. Then, the S_1-*keto* isomer undergoes a twisting geometry change, which facilitates the coupling of the S_1 state to the ground electronic state *via* another CI. Once in the S_0 state, OB undergoes *keto-enol* tautomerisation, which recovers the original *enol* species. Although Baker *et al.* [161] detected the presence of a long-lived photoproduct assigned to a *trans-keto* photoproduct in their TEAS measurements, the identification of this species would have been ambiguous without the complementary TVAS measurements, further discussed in Section 3.1.1. Indeed, the earlier study by Ignasiak *et al.* [201] assigned the long-lived species to the formation of phenoxyl radicals, which goes against the find-

ings of Baker *et al.* [161]. Notably, the relaxation pathway remained consistent, no matter whether the pump wavelength was in the UVA, UVB or UVC region [203]. The ultrafast relaxation mechanism proposed experimentally using TEAS was supported by non-adiabatic dynamics simulations by Li *et al.* [204]. Comprehensive diagrams pertaining to the relaxation of OB following UVA excitation have been published previously [65, 155, 161].

In reality, inorganic sunscreen filters (usually TiO_2 or ZnO if any) are often included in a completed formulation as a complement to their organic counterparts, to increase the levels of protection that a sunscreen can provide [205]. One previous TEAS study determined the influence of TiO_2 on the photodynamics of OB [206]; these results have been reviewed in detail previously [65]. In summary, although the excited state lifetime of TiO_2 varies according to concentration (femtosecond lifetimes at low concentrations, to beyond nanoseconds at high concentrations), the presence of TiO_2 did not affect the mechanism of action of OB in solution. From a photochemical perspective, we can deduce by combining these results that OB is almost the ideal sunscreen filter. Unfortunately its use is becoming more limited due to its adverse allergenic and environmental effects [48, 98, 207, 208].

The existence of safety and efficacy concerns for many UV filters including OB [209] highlights the importance of seeking new alternatives. Cinnamates have also been a popular choice for UVB protection in commercial sunscreens, particularly 2-ethylhexyl-*E*-4-methoxycinnamate (EHMC), which is approved by both the FDA and EU for this use [84]. However, EHMC undergoes *trans-cis* isomerisation upon exposure to UV radiation [210], with safety concerns existing particularly for the *cis* form [211, 212]. Hanson *et al.* [213] determined the quantum yields for *cis-trans* isomerisation upon solar irradiation to be 0.47 ± 0.06 in methanol and 0.60 (zero error to three significant figures quoted) in cyclohexane. For the reverse *trans-cis* isomerisation, the quantum yields were 0.37 ± 0.01 in methanol and 0.28 ± 0.01 in cyclohexane, therefore the potential exists for forming the harmful *cis* species on the skin, if a sunscreen containing EHMC is applied.

The TEAS/TR-IY study by Peperstraete *et al.* [197] on EHMC (reviewed previously by Baker *et al.* [159]) inspired the investigation by Woolley *et al.* [214] on the effect of additional functionalisation on the photostability of the cinnamate family of sunscreen molecules. This study sought to deepen the knowledge of the isomerisation that takes place within cinnamates, the subject of many previous studies [145–147, 197, 210, 215, 216]. Specifically, by adding an additional methyl acrylate moiety on to methyl cinnamate, structure shown in Figure 4, the effect of symmet-

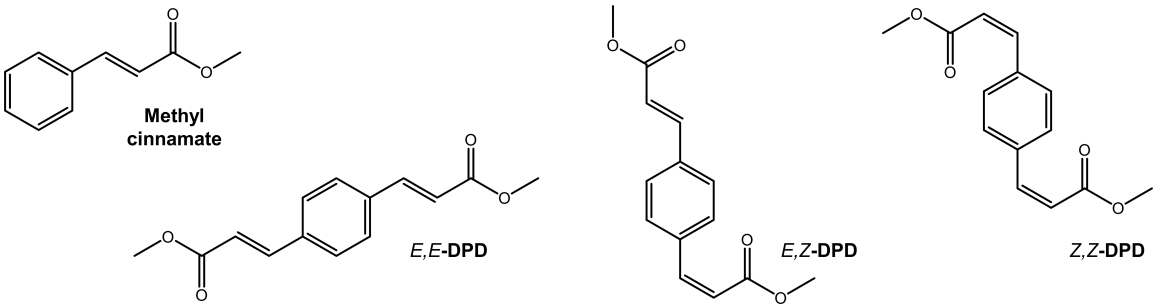

Figure 4. Molecular structures of the precursor molecule, methyl cinnamate, alongside the three geometric isomers synthesised by Woolley *et al.* [214] with an additional methyl acrylate moiety: *E,E*-DPD, *E,Z*-DPD and *Z,Z*-DPD.

rical functionalisation on the isomerisation of cinnamates could be investigated. The motivation for additional moieties is largely driven by alleviating safety concerns associated with *trans-cis* isomerisation, and the potential avoidance of known endocrine disruption characteristics and coral bleaching effects [96, 217]. The absorption could also be red-shifted to increase the UVA protection afforded by the molecule, perhaps by extension of the conjugation of the chromophore [218].

The study considers three geometric isomers: 3-3'-(1,4,phenylene)(2*E*, 2'*E*)-diacrylate, 3-3'-(1,4,phenylene)(2*Z*, 2'*E*)-diacrylate and 3-3'-(1,4,phenylene)(2*Z*, 2'*Z*)-diacrylate, abbreviated herein to *E,E*-DPD, *E,Z*-DPD and *Z,Z*-DPD respectively. Their structures are shown in Figure 4. One immediate benefit of *E,E*-DPD was that its absorption peak was red-shifted into the UVA region, where new options for inclusion in sunscreens are needed [69]. A range of solvents of different polarity and protic characteristics were chosen for the study by Woolley *et al.* [214]: acetonitrile, ethanol and cyclohexane, with the pump wavelength set to the UV-visible absorption maximum for *E,E*-DPD in the respective solvent.

Woolley *et al.* [214] conclude from this study that *E,E*-DPD evolves from the Franck-Condon region of the S_1 state on a comparable timescale (< 1 ps), to EHMC after the initial photoexcitation (τ_1, Figure 5). However, the length of time to traverse the S_1 potential energy surface through the S_1/S_0 CI and repopulate the S_0 state, representing the lifetime of isomerisation (to regenerate E,E-DPD or form E,Z-DPD), increased 5-fold in the *E,E*-DPD species ($\sim$10 ps) [214], compared to $\sim$2 ps for EHMC [197] (τ_2, Figure 5). This could be due to a restriction of movement of the molecule within the solvent caused by the additional methyl acrylate moiety, no matter the polarity of the solvent. Differences were also found between the decay pathway from the CI, specifically one single decay pathway was found for EHMC, towards formation of the higher energy *cis*-isomer photoproduct [197, 219] (τ_3, Figure 5(a)) but an additional pathway was found in DPD, made evident by an excited

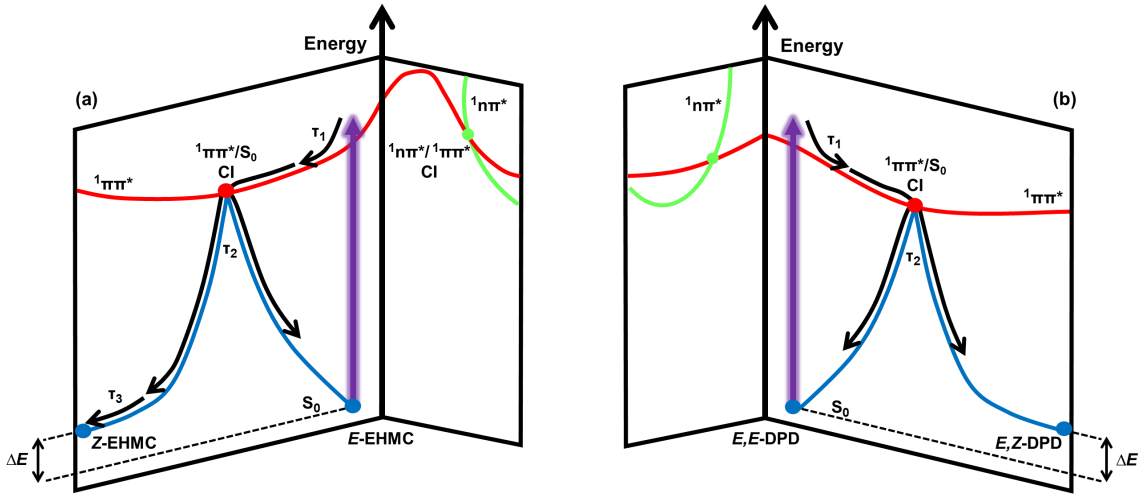

Figure 5. Relaxation schematic for (a) *E*-EHMC, based on the results presented in ref. [197], published by the PCCP Owner Societies (b) Comparable relaxation schematic for *E,E*-DPD, reproduced and adapted from the publication by Woolley *et al.* [214]. The authors add that τ_3 is omitted for clarity; it would correspond to trapped population in the $^1n\pi^*$ state and the *E,Z*-DPD species. Published by the PCCP Owner Societies.

state absorption feature at 400 nm that could not be assigned solely to a geometric isomer. The second pathway was assigned by Woolley *et al.* [214] to a separate state, either a triplet state, or a $^1n\pi^*$ state. The presence of $^1n\pi^*$ states have been reported to play a role in the photodynamics of similar systems [146, 147, 220, 221].

Through steady-state irradiation, *i.e.* exposing the molecules to equivalent solar fluences for a prolonged period (in this case two hours), Woolley *et al.* [214] determined that the absorbance of the *E,Z* species is spectrally blue-shifted compared to that of the *E,E* species; this blue shift was also predicted using computational methods [214]. Hence, the UVA protection afforded after isomerisation was decreased, analogous to EHMC. There was no evidence to suggest that the *Z,Z* species was present in any of the ultrafast experiments; this was corroborated using NMR after steady-state irradiation of the *E,E* species, therefore the photoequilibrium that is established upon excitation is only between the *E,E* and *E,Z* species.

However, as with all TEAS experiments, biological safety concerns such as endocrine disruption and photocontact dermatitis, cannot be addressed with this technique alone. Therefore, complementary studies such as endocrine disruption assays would offer additional beneficial insights. If these returned favourable results, then the molecular design emphasis of the study by Woolley *et al.* [214] could be used to adapt current sunscreen filters further, in order to enhance their photoprotection properties.

3.1.1. Future insights: probing vibrational states

To date, the OB study by Baker *et al.* [161] remains the only study to implement TVAS (see Section 1.2.3) for sunscreen applications specifically. This is somewhat surprising, given that TVAS can detect structural changes in a molecule, for example chemical bonds being formed or destroyed. Such changes are simply not possible to confirm by probing electronic states alone using TEAS, as mentioned in Section 1.2.3. As such, combining the two techniques is perhaps an area of exploration for future study, to investigate the relaxation pathways that may occur in sunscreen filters upon solar excitation more thoroughly. In the case of OB, TVAS was able to determine that the quantum yield of the photoproduct was around 10% [161]. A candidate for this long-lived species was also identified; a vibrationally hot *trans-keto* isomer formed upon *cis-trans* isomerisation [161]. Identifying this photoproduct would not have been possible without the structural information that TVAS provides. It may be the case that the *trans-keto* photoproduct could undergo subsequent *trans-cis* isomerisation to recover the original chelated *enol* species, although this was not observed by Baker *et al.* [161] due to the process not occurring within the temporal window of the experiment ($\sim$ 1.3 ns). Overall, although the lifetime of this long-lived photoproduct and its potential effects on the skin is unknown, the conclusion was made by Baker *et al.* [155, 200] that OB demonstrated the characteristics of a photophysically ideal sunscreen, because of its rapid decay to the ground state and broadband UV protection range, measured with a combination of TEAS, TVAS and steady-state UV-Vis spectroscopy.

3.2. *Sunscreens inspired by nature*

The current concerns surrounding existing organic UV filters are motivating formulators to turn to nature-inspired photoprotection for the next generation of sunscreens, to improve the compatibility with nature, both in terms of our skin and the natural environment [222, 223]. In this section of the review, the recent ultrafast spectroscopy studies of these new classes of sunscreen molecule, derived from plants and algae, will be discussed.

3.2.1. Plant-derived sunscreens: sinapates and derivatives in solution

Plants have developed protective barriers within the epidermis layer of their leaves, to prevent UV photodamage during sun exposure [224]. This photoprotective layer is analagous to melanin pigments in human skin, which prevent excessive UV radiation from reaching the DNA contained within skin cells [225, 226]. The laser spectroscopy

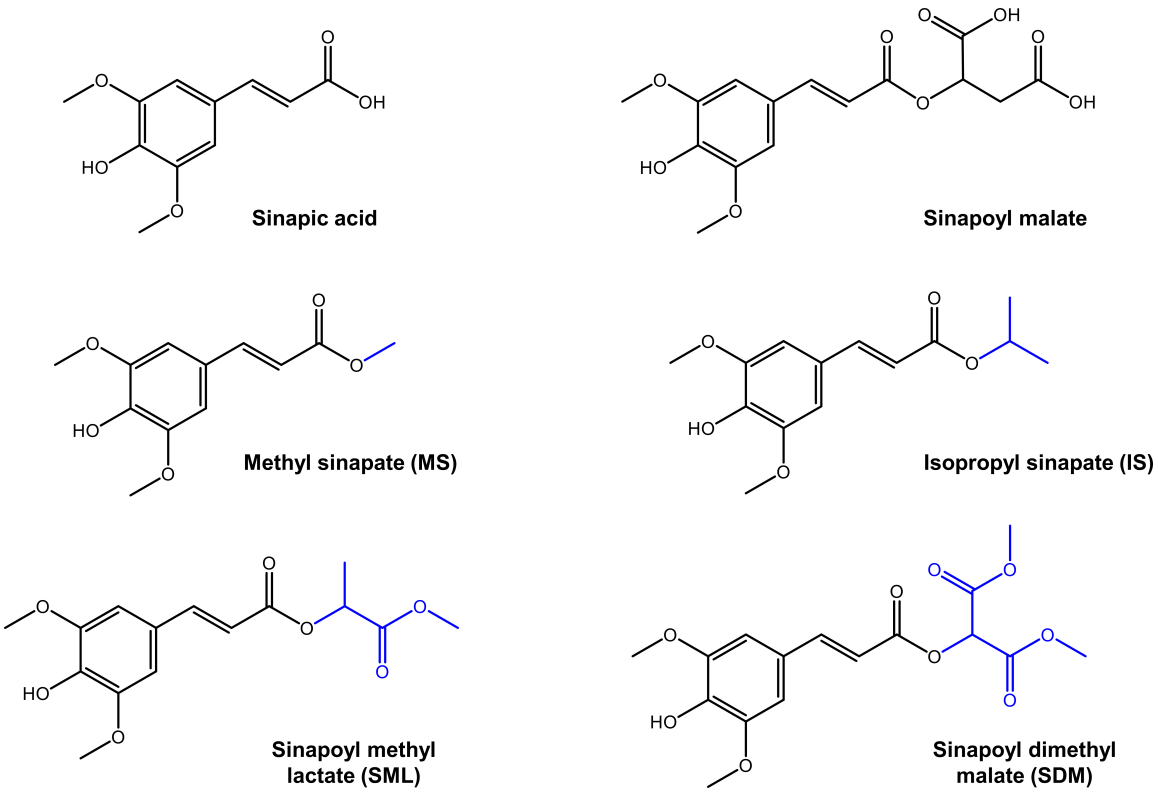

Figure 6. Structures of sinapic acid, sinapoyl malate (the ester found in plant leaves), and the four structures investigated by both Liu *et al.* [227] and Dean *et al.* [142]: methyl sinapate (MS), isopropyl sinapate (IS), sinapoyl methyl lactate (SML) and sinapoyl dimethyl malate (SDM), with the groups added to the sinapate ester moiety shown in blue for reference.

studies on so-called 'plant sunscreens' were pioneered by Zwier and co-workers in the frequency domain [142], and now serves as the inspiration behind many of the studies discussed herein.

TEAS was used to investigate the photodynamics of the photoprotection molecule and common metabolite sinapoyl malate, a sinapate ester that has been identified in the *Arabidopsis* plant, to determine its potential as a future sunscreen filter [228, 229]. A comprehensive review of these early studies into the ultrafast photodynamics of plant sunscreens has been published previously [155]. Since then, further TEAS studies have taken place on sinapoyl malate, which investigate more closely how the viscosity of a solvent can affect the *trans-cis* isomerisation relaxation pathway [230]. Briefly, these results showed that the timescales required for isomerisation to occur significantly increased with increasing solvent viscosity, from 47 ps in ethanol, to 560 ps in glycerol. It was concluded that the isomerisation resulted in a large amplitude vibrational motion, such as a traditional 'bond flip'. This motion would experience greater friction from the surrounding solvent molecules, and thus be impeded, accounting for the large increase in isomerisation lifetime [230]. Once again, these results have been reviewed in more detail in a previous publication [65].

Table 1. Time constants (τ_n) for isopropyl sinapate (IS), sinapoyl methyl lactate (SML) and sinapoyl dimethyl malate (SDM) in aqueous buffer solution with excitation (pump) wavelength of 320 nm, as determined by Liu *et al.* [227]. Table adapted with permission from ref. [227] © Elsevier

	IS	SML	SDM
τ_1 (ps)	0.25	0.26	0.18
τ_2 (ps)	1.04	0.87	0.77
τ_3 (ps)	9.96	12.2	7.19

The photodynamics of four more sinapate derivatives: methyl sinapate (MS), isopropyl sinapate (IS), sinapoyl methyl lactate (SML) and sinapoyl dimethyl malate (SDM), shown in Figure 6, have recently been explored using a combination of TEAS and time-dependent density functional theory (TD-DFT) techniques [227, 231]. These four structures were the central focus of the above-mentioned frequency-resolved gas-phase investigation by Dean *et al.* [142]. The results in solution discussed herein mark the next phase of the *bottom-up* approach: from gas-phase to solution.

The first part of the study by Liu *et al.* [227] sought to determine whether the size of the sinapate ester had any effect upon their *trans-cis* isomerisation pathways in aqueous buffer solution (0.1 M NaH_2PO_4, 0.1 M Na_2HPO_4, pH = 6.8). Notable features of the transient absorption spectra (TAS) by Liu *et al.* [227] are an excited state absorption feature (ESA) from 370 – 420 nm and a stimulated emission (SE) feature with a central wavelength of 485 nm, however the spectrum is not reproduced here.

The SE feature was assigned to fluorescence from the initially photoexcited S_1 state in all four cases. Both the positive and negative mΔOD features (Section 1.2.4) in all four molecules arrive to baseline at the same time. The authors determine that both features must result from the same state, in this case the S_1 state. From their data, Liu *et al.* [227] also assert that there is no evidence of dark $n\pi^*$ states, which can result in long excited-state lifetimes as seen in EHMC [149]; nor free radicals, which can indirectly incite DNA and protein damage in the skin [232]. A quantitative insight into these features, and the decay mechanism, was attained by extracting time constants using the software Glotaran, a Java-interface for the R package TIMP. The full details of how this program fits the data are explained in

Table 2. Time constants (τ_n) for methyl sinapate (MS) *in vacuo* and in four solvents: cyclohexane, dioxane, acetonitrile and methanol as determined by Baker *et al.* [229, 235], also MS in aqueous buffer solution and within a PVA film, as determined by Liu *et al.* [227]. λ_{pump} denotes the excitation (pump) wavelength for each experiment, which in each case is equivalent to the λ_{max} for each molecule

	Gas	Cyclohexane	Dioxane	Acetonitrile	Methanol	Buffer	Film
λ_{pump}	322	320	327	322	328	320	320
Ref.	[235]	[235]	[229]	[229]	[229]	[227]	[227]
τ_1 (ps)	3.1 ± 0.7	0.18†	0.12 ± 0.05	0.053†	0.65 ± 0.11	0.22‡	5.2‡
τ_2 (ps)	28 ± 8	3.06†	1.32 ± 0.16	0.54 ± 0.05	4.26 ± 0.90	0.70‡	175‡
τ_3 (ps)	> 1200*	9.22 ± 0.32	12.8 ± 1.3	18.0 ± 0.8	24.2 ± 1.5	7.69‡	-
τ_4 (ns)	-	> 2.5*	> 2.5*	> 2.5*	> 2.5*	-	-

* Outside the maximum time window of the instrument
† Errors on these measurements are within the instrument response (< 80 fs)
‡ No errors quoted

detail in separate publications [155, 233, 234]. It was found that all four datasets in buffer solution could be fitted with three time constants. These are shown in Table 1 for IS, SML and SDM and Table 2 for MS. The time constants τ_1 and τ_2 were assigned to multiple processes, namely intramolecular vibrational energy redistribution (IVR) and solvent rearrangement. Their evidence for these processes is spectral red-shift in the SE feature at early time delays (up to 2.1 ps). Finally, τ_3 is the time taken for the isomerisation to occur, which takes several picoseconds longer in SML compared to MS and SDM [227].

Overall, it was determined that the time constants had a non-linear dependence upon the size of the sinapate ester (in size order: MS < IS < SML < SDM, see Figure 6 for reference). However, all four compounds returned to the ground state faster than had been seen in previous studies of sinapoyl malate [229, 236]. Therefore, Liu *et al.* [227] propose that, at least in buffer solution, all four compounds display more favourable energy dissipation characteristics than sinapoyl malate, which could in turn be applicable for sunscreen use.

A recent study by Baker *et al.* [235] combined TR-IY (discussed in Section 2) and TEAS in a range of solvents to determine the photodynamics of MS, shown in Figure 6. TEAS measurements of MS in dioxane, acetonitrile and methanol can be found in an earlier publication by Baker *et al.* [229] and will also be discussed here. To begin

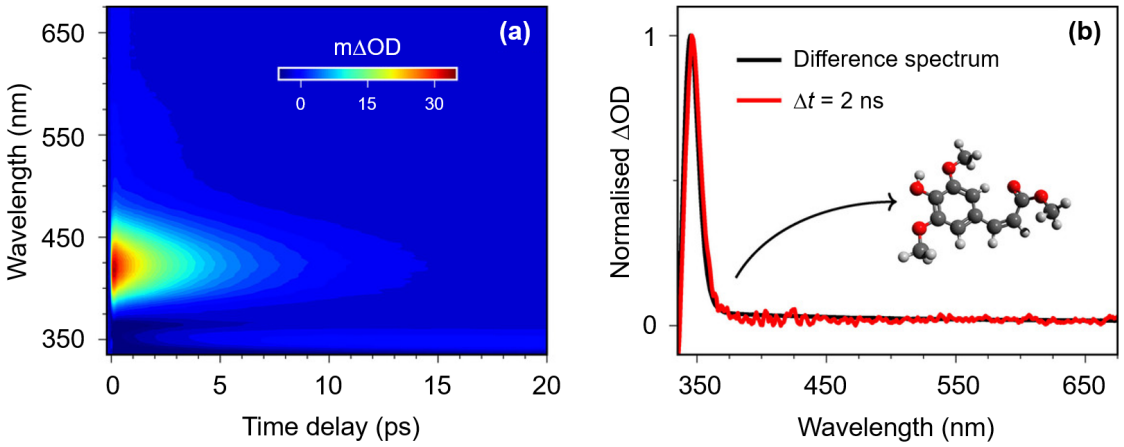

Figure 7. (a) False colour heat map of the TEAS spectrum of MS in cyclohexane ($\lambda_{\text{pump}} = 320$ nm). (b) Plot to show the TAS of MS in cyclohexane with a pump-probe time delay of 2 ns, compared to the UV-visible difference spectrum after irradiation of MS by UVA radiation for several hours. The correspondence of these two plots confirms the existence of the *cis*-isomer. Reproduced and adapted with permission from ref. [235] © Wiley-VCH Verlag GmbH & Co. KGaA

to understand the different quantitative insights that the two techniques provided in the study of MS, the time constants of the combined gas-solution phase study [235] alongside the additional solution-phase measurements [229], are shown in Table 2.

This review has highlighted that there are some differences in what was observed between the studies by Baker *et al.* [229, 235] and Liu *et al.* [227]. The time constants τ_1 to τ_3 are comparable in magnitude amongst all solvents, although the polarity of the solvent appears to have the largest effect on the *trans-cis* isomerisation. However, the presence of the *cis*-isomer photoproduct is not observed in the TEAS measurements taken by Liu *et al.* [227]. The publications by Baker *et al.* [229, 235] have measured the dynamics of MS in a large number of solvents and a photoproduct has been observed in each case, therefore it is unlikely that the solvent is preventing the detection of the *cis*-isomer. These results are also comparable to those observed by Horbury *et al.* [237] on ethyl ferulate in cyclohexane, a comparable plant-based molecule that also undergoes *trans-cis* isomerisation that can be detected using TEAS. Therefore, a potential explanation for the discrepancy could be due to the differences in probe windows. The shortest wavelength that Liu *et al.* [227] can resolve in their probe window is 380 nm, compared to 330 nm in the other studies [229, 235, 237]. As the *cis*-isomer can be detected on the spectral edge (335 nm) in ethyl ferulate and 360 nm in methyl sinapate (as shown in Figure 7), both of which are outside of the probe window for the study by Liu *et al.* [227], this may account for the discrepancy between them.

However, Liu *et al.* [227] could detect the *cis*-isomer during photostability tests of MS, IS, SML and SDM in the buffer solution. The photostability tests involved

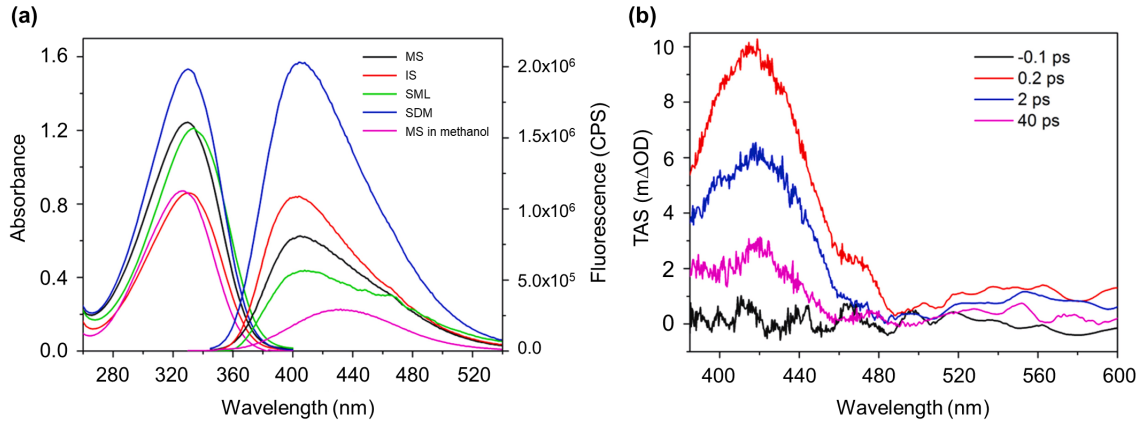

Figure 8. (a) Steady-state UV-visible absorption spectra and emission spectra (measured at 320 nm excitation) of MS, IS, SML and SDM in the PVA film, in addition to MS in methanol. (b) Wavelength evolution spectra of MS in PVA film (λ_{pump} = 320nm) at four different pump-probe time delays. Reproduced and adapted with permission from ref. [227] © Elsevier.

continuously irradiating the four molecules with UV light, then measuring a UV-visible absorption spectrum after one, five and ten minutes. A similar method was used by Horbury *et al.* in the study of the *E* and *Z* form of ethyl sinapate [238] and by Baker *et al.* for the attainment of the ΔUV-visible spectrum shown in Figure 7 [235]. All four molecules displayed similar changes in the UV-visible spectrum: an initial decrease in absorbance due to the formation of the *cis* isomer, which eventually becomes constant, suggesting an equilibrium between the two isomers.

3.2.2. Methyl sinapate in PVA films

Notably, Liu *et al.* [227] take an additional step towards simulating the effect of applying a sunscreen to the surface of the skin, by including the sinapate esters within a poly(vinyl alcohol) (PVA) hydrogel film. The process involved adding PVA (with degree of polymerisation ≈ 2000) into the aforementioned buffer solution containing each sinapate ester, followed by stirring (5 hours) and a drying process (6 hours at 308 K), thus leaving the molecule of interest dissolved within the PVA network [227]. PVA hydrogels have previously been shown to be a mimic for the skin's surface and other biological tissues such as heart valves, cartilage tissue and corneal implants [239]. They are also used for medical applications such as wound dressings [240].

In their steady-state UV-visible spectra shown in Figure 8(a), Liu *et al.* [227] observed a spectral red-shift of approximately 10 nm when each of the sinapate derivatives were dissolved into the film, with the peak of absorption now situated at 330 nm. The cause of this red-shift was assigned by the authors to the presence of the alcohol groups within the PVA film, due to the correspondence of the spectrum of MS in the film and in methanol solution. Conversely, the emission spectra were spec-

trally blue-shifted compared to the buffer solution. Although there was also a spectral blue-shift observed for MS in methanol compared to the buffer solution, it was not as profound as that of MS in the PVA film. Liu *et al.* [227] therefore postulated that additional factors must be affecting the emission of MS, aside from the presence of alcohol groups. The authors ultimately assigned the blue-shift to the restriction of movement of the sinapate esters due to the less mobile solvent environment. It is clear from these measurements that the surroundings have a direct impact upon the photodynamics of the potential plant sunscreens, *i.e.* the relaxation of the molecule following photoexcitation is altered [227, 230].

TEAS was also used to determine the ultrafast dynamics of methyl sinapate (MS) in the PVA film; selected wavelength evolution spectra for significant time delays are shown in Figure 8(b). The excited state absorption (ESA) feature dominates the dynamics between 380 – 450 nm, which the authors note is broader than the ESA observed in the buffer solution. Another significant difference between the TAS in buffer solution and the PVA film is the disappearance of the negative stimulated emission (SE) feature in the latter system [227]. One explanation for this could be the large spectral blue-shift of the emission spectrum of MS in the film, thus the ESA and SE features overlap. Once again, the presence of the long-lived photoproduct, assigned to the *cis*-isomer is not detected, for reasons discussed above pertaining to the spectral window of the probe.

Following quantitative data analysis, the TAS were again fitted using the methods devised by Snellenberg *et al.* [233], this time two time constants were elucidated: $\tau_1 = 5.2$ ps and $\tau_2 = 175$ ps (as shown in Table 2). Liu *et al.* [227] do not assign the shorter time constant τ_1 to a single process, instead a combination of intramolecular vibrational energy redistribution (IVR), solvent rearrangement and internal conversion within the excited state. This was also the case in the buffer solution, however the equivalent time constants were of the order of femtoseconds. The constant τ_2 was assigned to the *trans-cis* isomerisation motion, which the authors note is a 25-fold increase on the equivalent time constant in the buffer solution. The elongation of these time constants is further evidence for the restriction of motion in the film environment. This is similar to the observations made by Horbury *et al.* with sinapoyl malate in very viscous solvents (ethylene glycol and glycerol) [230].

The authors justify their use of PVA as a skin model due to the complex hydrogen bonding networks [227], however more complex models have been investigated as closer mimics of the epidermis [241]. This model combines PVA with polydimethyl siloxane (PDMS) to more closely represent the viscoelasticity, hydration and surface

properties of the skin. Therefore, opportunities remain for ultrafast spectroscopy techniques to continue to progress towards even more realistic skin models, in order to discern the effect that application of the product to the skin has upon its photodynamics.

3.2.3. Mycosporine amino acid motifs

Two additional classes of nature-derived sunscreens are mycosporines and mycosporine-like amino acids (MAAs). Mycosporines are fungal metabolites characterised by a cyclohexenone core (see Figure 9(c)). MAAs have also been identified within cyanobacteria, phytoplankton and plant-derived sources such as algae, and instead possess a cyclohexenimine core (see Figure 9(d)) [242–248]. Both mycosporines and MAAs are well-known for their UV protection properties in the systems from which they are extracted [249]. Mycosporines and MAAs have been used synonymously in the literature [250], therefore both classes of molecule will be referred to as MAAs herein. MAAs are being regarded as potential new sunscreen ingredients, owing to their ability to absorb radiation in the UVA region, a significant challenge that faces current sunscreens (as discussed in Section 1.1) [251]. Some MAAs, such as mycosporine-glycine (structure shown in Figure 9) also exhibit antioxidant properties, which along with their favourable photostability profile, would limit photodamage caused by sun overexposure [244, 252]. As such, their use is being explored for use in cosmetic products in industry [253].

Sampedro and co-workers have used *ab initio* methods to explore the photodynamics of MAAs and basic MAA scaffolds [254–258], in order to identify the simplest MAA-based compound that fulfilled the criteria for an efficient UV filter. In line with the *bottom-up* approach to the sunscreen work discussed thus far [119, 171] and inspired by the work of Losantos *et al.* [254], TEAS studies were conducted on two simplified chromophores (or motifs) of MAAs by Woolley *et al.* [259]: 3-aminocyclohex-2-en-1-one (termed ACyO) and (Z)-N-(3-(butylamino)-2-methylcyclohex-2-en-1-ylidene)butan-1-aminium 4-methylbenzenesulfonate (termed NN). The structures of both ACyO and NN, alongside the MAAs mycosporine-glycine and palythine on which these motifs are based, are shown in Figure 9. ACyO features a fundamental cyclohexenone core, with NN featuring the cyclohexenimine core. The UV-visible spectra of ACyO and NN are shown in Figure 9(a) and (b) respectively. These spectra indicate that the solvent environments are impacting upon molecular behaviour, perhaps due to their differing polarities. The absorption maximum of ACyO shifts from 272 nm in acetonitrile to 285 nm in methanol, although the spec-

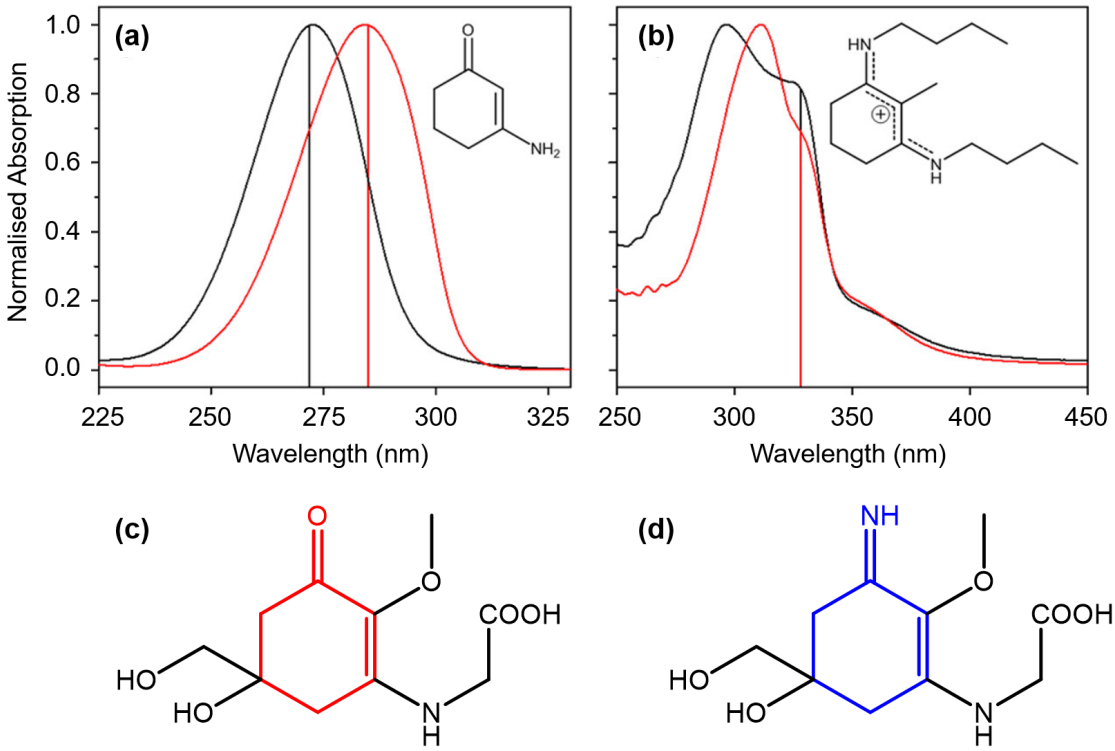

Figure 9. UV-visible absorption spectra of (a) ACyO and (b) NN (structures inset) in acetonitrile (black line) and methanol (red line), with the pump excitation wavelength (λ_{pump}) indicated by the vertical lines. Molecular structures of two MAAs are also shown: (c) mycosporine-glycine, with cyclohexenone core shown in red, and (d) palythine, with cyclohexenimine core shown in blue. Reproduced and adapted with permission from ref. [259] © ACS. Further permissions related to the material should be directed to the ACS.

tral shape and width remain very similar to one another (Figure 9(a)). For NN, the absorption peak in the UVA region (328 nm) has not shifted, however the spectrum has broadened and spectrally red-shifted in the UVB region in acetonitrile.

The TEAS measurements conducted by Woolley *et al.* [259] for the two MAA motifs in acetonitrile and methanol, with the corresponding TAS shown in Figure 10, show that solvent effects are more profound in ACyO (Figures 10(a), (b)) compared to NN (Figures 10(c), (d)). In fact, the TAS of NN do not display any apparent differences between the two solvents. The quantitative insights into the dynamical processes herein were attained through a global analysis using Glotaran, the fitting software mentioned on several occasions throughout Section 3 [233], with the elucidated time constants shown in Table 3. The first feature that both NN datasets have in common (see Figures 10(c), (d)) is the large coherent artefact around time zero [260]; the low intensity positive mΔOD signal that extends vertically from 0 ps across the entire probe region. These artefacts are caused by multiphoton interactions between the pump and probe pulses when they arrive at the sample simultaneously. These artefacts are discussed in detail in the publications by Ruckebusch *et al.* [158] and

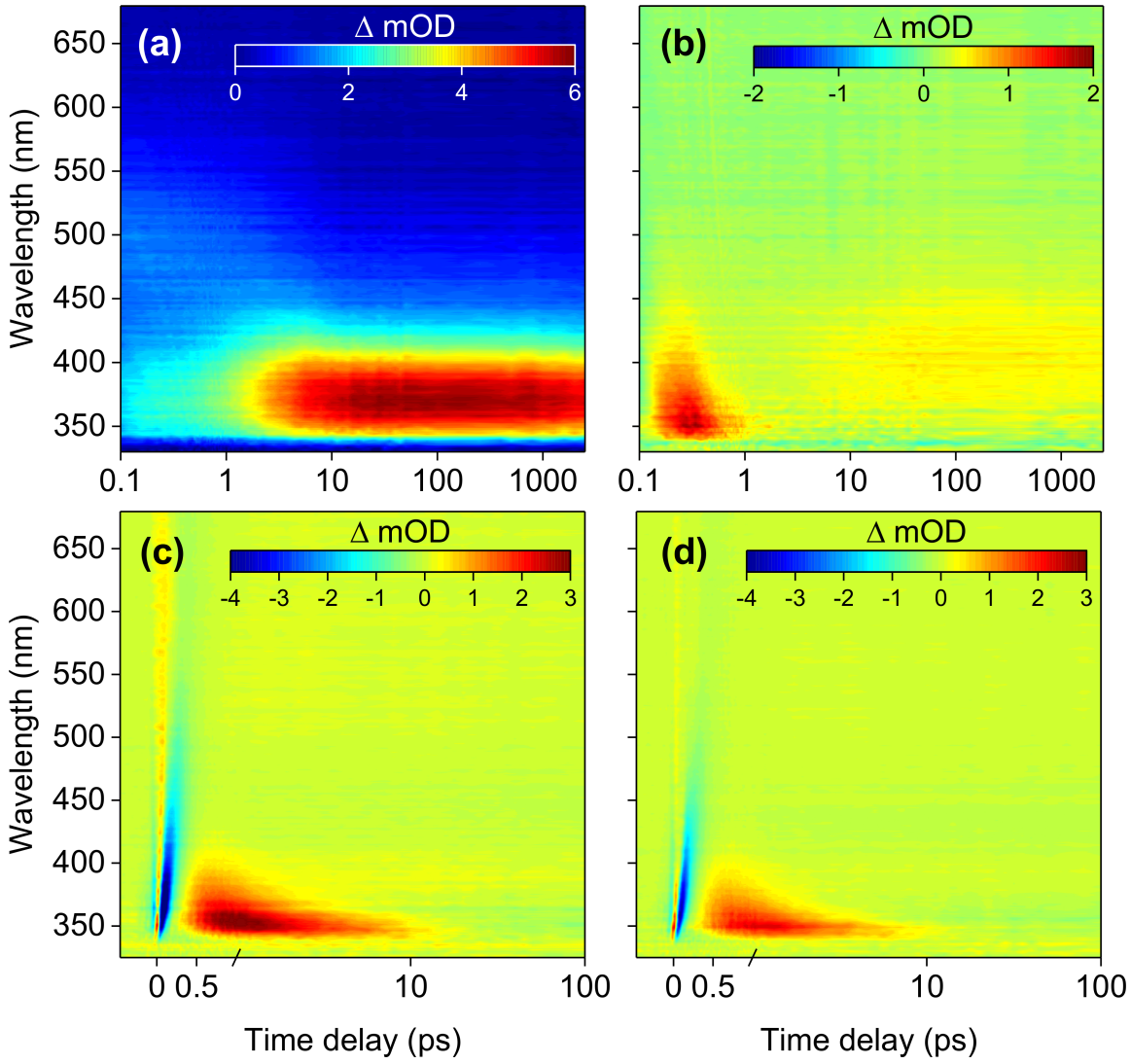

Figure 10. TAS displayed as a false colour heat map, of ACyO in (a) acetonitrile and (b) methanol, and of NN in (c) acetonitrile and (d) methanol. Note that for NN data, the time delay is plotted linearly up to 1 ps, and is on a logarithmic scale thereafter. Figures reproduced and adapted with permission from ref. [259] © ACS. Further permissions related to the material should be directed to the ACS.

Lorenc *et al.* [261]. In both cases, the coherent artefact is followed by an ESA feature centred at 350 nm, that extends up to 400 nm initially. Then, the ESA feature subsequently blue-shifts and decreases in spectral width, until it decays to zero after around 15 ps. Less prominent features include a GSB (centred at 340 nm) which is evident at time delays < 1 ps, and an SE feature that is observed between 400 nm and the edge of the probe region (680 nm). To interpret these TAS features, Woolley *et al.* were able to attain significant insights from the quantum dynamics studies by Losantos *et al.* [254], despite the calculated potential energy surfaces not being for identical systems to those studied experimentally. The first time constant (τ_1, see Table 3) was attributed to a geometry relaxation of the S_1 state with some

Table 3. Time constants for ACyO and NN in acetonitrile and methanol, as determined by Woolley *et al.* [259]. Table reproduced with permission from ref. [259] © ACS. Further permissions related to this material should be directed to the ACS.

	τ_1	τ_2	τ_3
ACyO			
Acetonitrile	2.80 ± 0.2 ps	$\gg$ 2.5 ns*	
Methanol	330 ± 40 fs	3.40 ± 0.3 ps	$\gg$ 2.5 ns*
NN			
Acetonitrile	440 ± 40 fs	2.49 ps ± 40 fs	$\gg$ 2.5 ns*
Methanol	680 ± 40 fs	1.52 ps ± 100 fs	$\gg$ 2.5 ns*

* Outside the maximum time window of the instrument

solvent rearrangement, alongside the movement of the excited state population to the S_1/S_0 CI. A spectral red-shift of the SE that may be expected due to movement along the potential energy surface is not immediately apparent, likely due to overlap of the ESA feature [259]. As these features manifest in TEAS as positive and negative signals respectively, any overlap would reduce the overall magnitude of the signal. The second time constant (τ_2) refers to the decay of the vibrationally hot S_0 state, and the third (τ_3) is representative of the formation of an additional species, which persists beyond the time window of the experiment. This could be a triplet state or the appearance of a photoproduct.

In contrast to NN, the TAS features of ACyO are not comparable between solvents and therefore will be discussed separately. For ACyO in acetonitrile (Figure 10(a)), there is a broad ESA feature initially that spans the range 340 – 600 nm. Within 6 ps, this evolves to a narrowing ESA feature (340 – 450 nm) that is spectrally blue-shifting, which persists beyond the maximum time window of the experiment of 2.5 ns. *Ab initio* calculations by Sui *et al.* [262] of ACyO in acetonitrile showed that excitation at the UV peak maximum would incite a $^1\pi\pi^*$ transition that populates the S_1 state. The first time constant (τ_1, see Table 3) was assigned to a vibrationally hot S_1 state population that evolves to a trapped population in the S_1 minimum. The lifetime of this vibrationally cold population is the process assigned to τ_2. Like NN, the populated states could be assigned more precisely by comparing experimental results to the recent *ab initio* calculations of Losantos *et al.* [254]. As the molecule traverses the S_1 potential energy surface, the molecule evolves from the initially populated

Franck-Condon region (which, according to Losantos *et al.* is on the S_2 surface which subsequently populates the S_1 state through a S_2/S_1 CI), continuously losing energy to the surrounding solvent. This means that the molecule becomes trapped in the minimum of the S_1 state, lacking the energy required to overcome the barrier to the S_1/S_0 CI.

Conversely for ACyO in methanol (Figure 10(b)), there is an initial ESA feature centred at 350 nm, which decays within 1 ps and almost returns to baseline. After 15 ps, a second ESA feature appears, albeit less intense, centred at around 400 nm that persists beyond 2.5 ns. An additional time constant was required to provide an adequate fit for this data (see Table 3). For this system, τ_1 was assigned by Woolley *et al.* [259] to a solvent rearrangement and geometry relaxation on the S_1 state. Then, τ_2 is assigned to vibrational cooling *via* vibrational energy transfer to the surrounding solvent, although this process was more efficient in acetonitrile. During this time, the evolving Franck-Condon region encounters a section along the S_1 potential energy surface where there is very little ESA; alternatively, both ESA and SE may be occurring concurrently. Either of these scenarios would account for the incidence of zero signal after a few hundred femtoseconds. Once again, this vibrational relaxation ensures that the molecule reaches the minimum of the S_1 state, τ_3 refers to the fact that ACyO cannot overcome the energy barrier within the time window of the experiment.

To summarise, Woolley *et al.* [259] corroborate the previous theoretical work conducted by Losantos *et al.* [254]. There was a barrier to the CI in the ACyO species, which prevents repopulation of the ground state, in contrast to the dynamics observed for the NN species. Therefore, it would be expected that mycosporines, which possess the cyclohexenone core, would not be favourable sunscreen candidates. The long-lived excited state observed could increase the likelihood of potentially harmful photochemical reactions taking place. However, it has been reported that the mycosporine gadusol demonstrates high levels of photostability in solution [263]. Therefore, the effect of additional groups on the cyclohexenone core unit should be investigated further, in order to identify beneficial modification that may facilitate an accessible S_1/S_0 CI.

4. Beyond the Solution-phase: Towards a Full Formulation

Solution-phase transient absorption studies, including those discussed in Section 3, have been invaluable for understanding the effects of solvent environment on the photodynamics of single current and potential UV filters. However, the possibility

remains that such simple models cannot predict how relaxation mechanisms of UV filters might be altered in a formulation setting. Baker *et al.* [206] published the first transient absorption spectra of two UV filters combined in solution: one organic and one inorganic (oxybenzone and TiO_2 respectively, discussed in Section 3.1). Although the photodynamics of oxybenzone appeared to be independent of the presence of TiO_2, such a result may not hold true for all pairings. For example, evidence exists to suggest that TiO_2 may induce additional photodegradation in avobenzone [264]. Furthermore, it is known that the photostability of the UVA filter avobenzone can be improved or detrimentally impacted by the presence of additional organic UV filters [84, 86–89]. Completed sunscreens consist of several UV filters, in addition to emulsifiers, emollients, surfactants and rheology modifiers, amongst other ingredients [46]. With this in mind, there is added potential for interaction between UV filters and ingredients within a full formulation.

The study by Liu *et al.* [227] attempted to model the photodynamics of plant-based UV filters on the skin's surface and measure them using TEAS, as discussed in Section 3.2.2. However, this study did not account for the influences of other sunscreen ingredients. Therefore, the scope to more closely mimic realistic conditions in TEAS experiments remains extensive. Potential ideas include: (i) temperature-resolved measurements to account for the temperature of the skin's surface, (ii) determining the effect of application of a product to the skin, *via* the use of synthetic skin substrates used in industry, and (iii) measuring the photodynamics of UV filters occurring within complex emulsions.

From experience within our laboratory, experimental challenges should be anticipated with progression towards real-life conditions. For example, as the number of components in the mixture increase and sample substrates become more realistic, more spectral features in each TAS will need to be deconvolved. It is essential therefore that the dynamics of the components have been fully characterised in a simpler environment, so that their behaviours in mixtures can be better understood, offering justification for the *bottom-up* approach.

The potential of ultrafast spectroscopy for sunscreen applications may not be limited to molecules that solely act as UV filters. Nowadays, there is added emphasis on making multi-purpose cosmetic components, for example UV filters with antioxidant properties [265, 266]. Antioxidants are often added to cosmetic products to quench reactive oxygen species that may induce photoaging [267]. Perhaps preferred characteristics of excited-state dynamics of such molecules could be identified using the techniques discussed in this review. Further scope also exists for developing a molecule

that effectively protects the skin from visible and infrared light, as well as UV light, which is of current industrial concern [268]. It has been found that the skin suffers from deleterious effects caused by blue light exposure [269], from sources such as mobile phones and computer screens. Studies thus far have focused upon these biological effects [270–272]; however, there is potential for ultrafast spectroscopy techniques to be used to inform the design of blue light absorbers, given their success at doing so for UV filters.

5. Conclusions and Outlook

Sunscreens have been developed as an artificial barrier against the deleterious effects of overexposure to UV radiation in humans. Although copious numbers of commercially available sunscreen products already exist, many challenges remain for sunscreen formulators. These challenges include: ensuring that sunscreen products offer their maximum photoprotection for many hours following sun exposure; formulating a homogeneous blend that is aesthetically pleasing to the consumer; and avoiding adverse effects being induced to consumers and the environment. As well as providing a reflection on the current challenges towards the creation of the 'ideal' sunscreen, this review explores the role of femtosecond pump-probe spectroscopy techniques to study fundamental behaviours of current and potential UV filters. In particular, the contributions of gas- and solution-phase time-resolved ultrafast spectroscopy to determine whether candidate sunscreen filters dissipate incident UV energy safely have been discussed, as well as the merits of implementing a *bottom-up* approach. The discussion begins with gas-phase techniques that study molecules in vacuum; followed by the effects of dissolving current and potential (*e.g.* nature inspired) UV filters in a wide range of solvents, towards the ability to determine the photodynamics of complex sunscreen matrices under realistic conditions. In parallel, the possibility of implementing molecular design, from simple motifs to full sunscreen molecules is explored, towards optimising properties for the next generation of sunscreens.

This review advocates that ultrafast spectroscopy offers an unprecedented insight into the initial fundamental behaviours of sunscreen constituents (particularly UV filters). Furthermore, this review has demonstrated the possibility of optimising a molecule's functional groups for optimum sunscreen performance. By exploring the capabilities of these spectroscopic techniques alongside longer-term (steady-state) experiments and more widely commercially accepted *in vitro* and *in vivo* techniques, it should be possible to characterise the expected behaviours of a sunscreen constituent. Using this knowledge, ingredients could perhaps be tailor-made to satisfy

requirements. The possibilities are not only limited to sunscreens. Opportunities also exist to extend the scope of ultrafast spectroscopy for cosmetic applications beyond sunscreens, *e.g.* for the testing of blue light filters and singlet oxygen quenchers that are currently being developed.

Acknowledgements

E.L.H. thanks the Engineering and Physical Sciences Research Council (EPSRC) for a PhD studentship through the EPSRC Centre for Doctoral Training in Molecular Analytical Science, grant number EP/L015307/1. V.G.S. is grateful to the Royal Society and the Leverhulme Trust for a Royal Society Leverhulme Trust Senior Research Fellowship, as well as the EU for a HO2020 FET-OPEN Grant entitled BoostCrop for financial support.

Disclosure statement

The authors have no conflicts of interest to declare.

References

[1] J. Nash, P. R. Tanner, and P. J. Matts, Dermatol. Clin. **24** (1), 63 (2006). <https://www.derm.theclinics.com/article/S0733-8635(05)00103-8/abstract>.

[2] J. E. Frederick, H. E. Snell, and E. K. Haywood, Photochem. Photobiol. **50** (4), 443 (1989). <https://doi.org/10.1111/j.1751-1097.1989.tb05548.x>.

[3] Y. Matsumi and M. Kawasaki, Chem. Rev. **103** (12), 4767 (2003). <https://doi.org/10.1021/cr0205255>.

[4] J. F. Bornman, P. W. Barnes, S. A. Robinson, C. L. Ballaré, S. D. Flint, and M. M. Caldwell, Photochem. Photobiol. Sci. **14**, 88 (2015). <http://dx.doi.org/10.1039/C4PP90034K>.

[5] J. R. Herman and E. A. Celarier, J. Geophys. Res.-Atmos. **102** (D23), 28003 (1997). <https://agupubs.onlinelibrary.wiley.com/doi/abs/10.1029/97JD02074>.

[6] R. L. McKenzie, P. J. Aucamp, A. F. Bais, L. O. Björn, and M. Ilyas, Photochem. Photobiol. Sci. **6**, 218 (2007). <http://dx.doi.org/10.1039/B700017K>.

[7] A. F. Bais, G. Bernhard, R. L. McKenzie, P. J. Aucamp, P. J. Young, M. Ilyas, P. Jöckel, and M. Deushi, Photochem. Photobiol. Sci. **18**, 602 (2019). <http://dx.doi.org/10.1039/C8PP90059K>.

[8] N. D. Paul and D. Gwynn-Jones, Trends Ecol. Evol. **18** (1), 48 (2003). <http://www.sciencedirect.com/science/article/pii/S0169534702000149>.

[9] J. B. Kerr and V. E. Fioletov, Atmos. Ocean **46** (1), 159 (2008). <https://doi.org/10.3137/ao.460108>.

[10] A. Mithal, D. A. Wahl, J. P. Bonjour, P. Burckhardt, B. Dawson-Hughes, J. A. Eisman, G. El-Hajj Fuleihan, R. G. Josse, P. Lips, and J. Morales-Torres, Osteoporos. Int. **20** (11), 1807 (2009). <https://doi.org/10.1007/s00198-009-0954-6>.

[11] P. Lips and N. M. van Schoor, Best Pract. Res. Clin. Endocrinol. Metab. **25** (4), 585 (2011). <http://www.sciencedirect.com/science/article/pii/S1521690X11000418>.

[12] A. Wirz-Justice, P. Graw, K. Kräuchi, A. Sarrafzadeh, J. English, J. Arendt, and L. Sand, J. Affect. Disord. **37** (2), 109 (1996). <https://doi.org/10.1016/0165-0327(95)00081-X>.

[13] M. B. Humble, J. Photoch. Photobio. B **101** (2), 142 (2010). <http://www.sciencedirect.com/science/article/pii/S1011134410001879>.

[14] R. M. Lucas, S. Yazar, A. R. Young, M. Norval, F. R. de Gruijl, Y. Takizawa, L. E. Rhodes, C. A. Sinclair, and R. E. Neale, Photochem. Photobiol. Sci. **18**, 641 (2019). <http://dx.doi.org/10.1039/C8PP90060D>.

[15] M. F. Holick, Anticancer Res. **36** (3), 1345 (2016). <http://ar.iiarjournals.org/content/36/3/1345.short>.

[16] P. H. Hart, M. Norval, S. N. Byrne, and L. E. Rhodes, Annu. Rev. Pathol. **14** (1), 55 (2019). <https://doi.org/10.1146/annurev-pathmechdis-012418-012809>.

[17] G. J. Fisher, Z. Wang, S. C. Datta, J. Varani, S. Kang, and J. J. Voorhees, New Engl. J. Med **337** (20), 1419 (1997). <https://doi.org/10.1056/NEJM199711133372003>.

[18] R. P. Gallagher and T. K. Lee, Prog. Biophys. Mol. Bio. **92** (1), 119 (2006). <https://www.sciencedirect.com/science/article/pii/S0079610706000137>.

[19] M. Wlaschek, I. Tantcheva-Poór, L. Naderi, W. Ma, L. A. Schneider, Z. Razi-Wolf, J. Schüller, and K. Scharffetter-Kochanek, J, Photoch. Photobio. B **63** (1), 41 (2001). <http://www.sciencedirect.com/science/article/pii/S1011134401002019>.

[20] H. R. Taylor, S. K. West, F. S. Rosenthal, B. Muñoz, H. S. Newland, H. Abbey, and E. A. Emmett, New Engl. J. Med. **319** (22), 1429 (1988). <https://doi.org/10.1056/NEJM198812013192201>.

[21] F. R. De Gruijl, Eur. J. Cancer **35** (14), 2003 (1999). <https://doi.org/10.1016/S0959-8049(99)00283-X>.

[22] D. L. Narayanan, R. N. Saladi, and J. L. Fox, Int. J. Dermatol. **49** (9), 978 (2010). <https://onlinelibrary.wiley.com/doi/full/10.1111/j.1365-4632.2010.04474.x>.

[23] P. A. Morganroth, H. W. Lim, and C. T. Burnett, Am. J. Lifestyle Med. **7** (3), 168 (2013). <https://doi.org/10.1177/1559827612460499>.

[24] M. Šitum, M. Buljan, V. Bulat, L. Lugović Mihić, Ž. Bolanča, and D. Šimić, Collegium Antropol. **32** (2), 167 (2008).

[25] J. Schmitt, A. Seidler, T. L. Diepgen, and A. Bauer, Brit. J. Dermatol. **164** (2), 291 (2011). <https://onlinelibrary.wiley.com/doi/abs/10.1111/j.1365-2133.2010.10118.x>.

[26] R. P. Gallagher, B. Ma, D. I. McLean, C. P. Yang, V. Ho, J. A. Carruthers, and L. M. Warshawski, J. Am. Acad. Dermatol. **23** (3), 413 (1990). <https://doi.org/10.1016/0190-9622(90)70234-9>.

[27] B. K. Armstrong and A. Kricker, J, Photoch. Photobio. B **63** (1), 8 (2001). <http://www.sciencedirect.com/science/article/pii/S1011134401001981>.

[28] M. R. Gailani, D. J. Leffell, A. M. Ziegler, E. G. Gross, D. E. Brash, and A. E. Bale, J. Natl. Cancer Inst. **88** (6), 349 (1996). <http://dx.doi.org/10.1093/jnci/88.6.349>.

[29] J. Cadet and T. Douki, Photochem. Photobiol. Sci. **17**, 18161841 (2018). <http://dx.doi.org/10.1039/C7PP00395A>.

[30] A. R. Rhodes, Cancer **75** (S2), 613 (1995). <https://onlinelibrary.wiley.com/doi/abs/10.1002/1097-0142%2819950115%2975%3A2%2B%3C613%3A%3AAID-CNCR2820751403%3E3.0.CO%3B2-G>.

[31] A. C. Geller, R. W. Clapp, A. J. Sober, L. Gonsalves, L. Mueller, C. L. Christiansen, W. Shaikh, and D. R. Miller, J. Clin. Oncol. **31** (33), 4172 (2013). <https://doi.org/10.1200/JCO.2012.47.3728>.

[32] Z. Apalla, A. Lallas, E. Sotiriou, E. Lazaridou, and D. Ioannides, Dermatol. Pract. Concept. **7** (2), 1 (2017).

[33] S. Solomon, D. J. Ivy, D. Kinnison, M. J. Mills, R. R. Neely, and A. Schmidt, Science **353** (6296), 269 (2016). <http://science.sciencemag.org/content/353/6296/269>.

[34] A. F. Bais, R. M. Lucas, J. F. Bornman, C. E. Williamson, B. Sulzberger, A. T. Austin, S. R. Wilson, A. L. Andrady, G. Bernhard, R. L. McKenzie, P. J. Aucamp, S. Madronich, *et al.*, Photochem. Photobiol. Sci. **17**, 127 (2018). <http://dx.doi.org/10.1039/C7PP90043K>.

[35] A. R. Ravishankara, J. S. Daniel, and R. W. Portmann, Science **326** (5949), 123 (2009). <http://science.sciencemag.org/content/326/5949/123>.

[36] J. B. Kerr and C. T. McElroy, Science **262** (5136), 1032 (1993). <https://science.sciencemag.org/content/262/5136/1032>.

[37] A. F. Bais, R. L. McKenzie, G. Bernhard, P. J. Aucamp, M. Ilyas, S. Madronich, and K. Tourpali, Photochem. Photobiol. Sci. **14**, 19 (2015). <http://dx.doi.org/10.1039/C4PP90032D>.

[38] G. Kelfkens, F. R. de Gruijl, and J. C. van der Leun, Photochem. Photobiol. **52** (4), 819 (1990). <https://onlinelibrary.wiley.com/doi/abs/10.1111/j.1751-1097.1990.tb08687.x>.

[39] R. P. Kane, Int. J. Climatol. **18** (4), 457 (1998). <https://rmets.onlinelibrary.wiley.com/doi/abs/10.1002/%28SICI%291097-0088%2819980330%2918%3A4%3C457%3A%3AAID-JOC242%3E3.0.CO%3B2-%23>.

[40] K. E. Burke and H. Wei, Toxicol. Ind. Health **25** (4–5), 219 (2009). <https://doi.org/10.1177/0748233709106067>.

[41] N. A. Kasparian, J. K. McLoone, and B. Meiser, J. Behav. Med. **32** (5), 406 (2009). <https://doi.org/10.1007/s10865-009-9219-2>.

[42] U. Osterwalder and B. Herzog, Photochem. Photobiol. Sci. **9**, 470 (2010). <http://dx.doi.org/10.1039/B9PP00178F>.

[43] M. E. Burnett, J. Y. Hu, and S. Q. Wang, Dermatol. Ther. **25** (3), 244 (2012). <https://onlinelibrary.wiley.com/doi/abs/10.1111/j.1529-8019.2012.01503.x>.

[44] U. Osterwalder and B. Herzog, Br. J. Dermatol. **161** (S3), 13 (2009). <https://onlinelibrary.wiley.com/doi/abs/10.1111/j.1365-2133.2009.09506.x>.

[45] R. Jansen, U. Osterwalder, S. Q. Wang, M. Burnett, and H. W. Lim, J. Am. Acad. Dermatol. **69** (6), 867.e1 (2013). <http://www.sciencedirect.com/science/article/pii/S0190962213008955>.

[46] U. Osterwalder, M. Sohn, and B. Herzog, Photodermatol. Photoimmunol. Photomed. **30** (2–3), 62 (2014). <https://doi.org/abs/10.1111/phpp.12112>.

[47] M. Lodén, H. Beitner, H. Gonzalez, D. Edström, U. Åkerström, J. Austad, I. Buraczewska-Norin, M. Matsson, and H. Wulf, Br. J. Dermatol. **165** (2), 255 (2011). <https://onlinelibrary.wiley.com/doi/abs/10.1111/j.1365-2133.2011.10298.x>.

[48] M. E. Burnett and S. Q. Wang, Photodermatol. Photoimmunol. Photomed. **27** (2), 58 (2011). <https://onlinelibrary.wiley.com/doi/abs/10.1111/j.1600-

0781.2011.00557.x>.

[49] J. B. Mancuso, R. Maruthi, S. Q. Wang, and H. W. Lim, Am. J. Clin. Dermatol. **18** (5), 643 (2017). <https://doi.org/10.1007/s40257-017-0290-0>.

[50] S. Schauder and H. Ippen, Contact Dermatitis **37** (5), 221 (1997). <https://doi.org/10.1111/j.1600-0536.1997.tb02439.x>.

[51] T. Wong and D. Orton, Clin. Dermatol. **29** (3), 306 (2011). <http://www.sciencedirect.com/science/article/pii/S0738081X10002105>.

[52] A. C. de Groot and D. W. Roberts, Contact Dermatitis **70** (4), 193 (2014). <https://onlinelibrary.wiley.com/doi/full/10.1111/cod.12205>.

[53] H. Hönigsmann, Photodermatol. Photoimmunol. Photomed. **18** (2), 75 (2002). <https://doi.org/10.1034/j.1600-0781.2002.180204.x>.

[54] A. R. Young, J. Claveau, and A. B. Rossi, J. Am. Acad. Dermatol. **76** (3, Supplement 1), S100 (2017). <http://www.sciencedirect.com/science/article/pii/S0190962216308805>, Challenges in photoprotection.

[55] J. A. Parrish, K. F. Jaenicke, and R. R. Anderson, Photochem. Photobiol. **36** (2), 187 (1982). <https://onlinelibrary.wiley.com/doi/abs/10.1111/j.1751-1097.1982.tb04362.x>.

[56] B. L. Diffey, C. T. Jansén, F. Urbach, and H. C. Wulf, Photodermatol. Photoimmunol. Photomed. **13** (1–2), 64 (1997). <https://onlinelibrary.wiley.com/doi/abs/10.1111/j.1600-0781.1997.tb00110.x>.

[57] K. Waterston, L. Naysmith, and J. L. Rees, J. Invest. Dermatol. **123** (5), 958 (2004). <http://www.sciencedirect.com/science/article/pii/S0022202X15320212>.

[58] L. Ferrero, M. Pissavini, and O. Doucet, Photochem. Photobiol. Sci. **9**, 540 (2010). <http://dx.doi.org/10.1039/B9PP00183B>.

[59] M. Pissavini, C. Tricaud, G. Wiener, A. Lauer, M. Contier, L. Kolbe, C. Trullás Cabanas, F. Boyer, V. Nollent, E. Meredith, E. Dietrich, and P. J. Matts, Int. J. Cosmet. Sci **40** (3), 263 (2018). <https://doi.org/10.1111/ics.12459>.

[60] M. Rohr, E. Klette, S. Ruppert, R. Bimzcok, B. Klebon, U. Heinrich, H. Tronnier, W. Johncock, S. Peters, F. Pflücker, T. Rudolph, H. Flösser-Müller, *et al.*, Skin Pharmacol. Physiol. **23** (4), 201 (2010).

[61] A. Dimitrovska Cvetkovska, S. Manfredini, P. Ziosi, S. Molesini, V. Dissette, I. Magri, C. Scapoli, A. Carrieri, E. Durini, and S. Vertuani, Int. J. Cosmet. Sci **39** (3), 310 (2017). <https://onlinelibrary.wiley.com/doi/abs/10.1111/ics.12377>.

[62] B. P. Binks, P. D. Fletcher, A. J. Johnson, I. Marinopoulos, J. Crowther, and M. A. Thompson, J. Photoch. Photobio. A **333**, 186 (2017). <http://www.sciencedirect.com/science/article/pii/S1010603016307468>.

[63] A. Springsteen, R. Yurek, M. Frazier, and K. F. Carr, Anal. Chim. Acta **380** (2), 155 (1999). <http://www.sciencedirect.com/science/article/pii/S0003267098005777>.

[64] A. W. Schmalwieser, S. Wallisch, and B. Diffey, Photochem. Photobiol. Sci. **11**, 251 (2012). <http://dx.doi.org/10.1039/C1PP05271C>.

[65] N. d. N. Rodrigues and V. G. Stavros, Sci. Prog. **101** (1), 8 (2018). <https://doi.org/10.3184/003685018X15166183479666>.

[66] S. Q. Wang, J. W. Stanfield, and U. Osterwalder, J. Am. Acad. Dermatol. **59** (6), 934 (2008). <http://www.sciencedirect.com/science/article/pii/S0190962208009341>.

[67] B. Diffey, Int. J. Cosmet. Sci. **31** (1), 63 (2009). <https://onlinelibrary.wiley.com/doi/abs/10.1111/j.1468-2494.2008.00471.x>.

[68] B. L. Diffey, P. R. Tanner, P. J. Matts, and J. F. Nash, J. Am. Acad. Dermatol. **43** (6), 1024 (2000). <http://www.sciencedirect.com/science/article/pii/S0190962200292529>.

[69] S. Q. Wang, H. Xu, J. W. Stanfield, U. Osterwalder, and B. Herzog, J. Am. Acad. Dermatol. **77** (1), 42 (2017). <http://www.sciencedirect.com/science/article/pii/S019096221730035X>.

[70] E. Q. Coyne, M. K. Lichtman, J. Simons, A. K. Sarkar, and T. M. Rünger, J. Am. Acad. Dermatol. **79** (2), 373 (2018). <http://www.sciencedirect.com/science/article/pii/S0190962218300227>.

[71] P. J. Matts, V. Alard, M. W. Brown, L. Ferrero, H. Gers-Barlag, N. Issachar, D. Moyal, and R. Wolber, Int. J. Cosmet. Sci **32** (1), 35 (2010). <https://onlinelibrary.wiley.com/doi/abs/10.1111/j.1468-2494.2009.00542.x>.

[72] D. Moyal, Expert Rev. Dermatol. **3** (3), 307 (2008). <https://doi.org/10.1586/17469872.3.3.307>.

[73] A. Fourtanier, D. Moyal, and S. Seite, Photochem. Photobiol. Sci. **11**, 81 (2012). <http://dx.doi.org/10.1039/C1PP05152K>.

[74] BASF Sunscreen Simulator 2019. <https://www.sunscreensimulator.basf.com/Sunscreen_Simulator/login>.

[75] B. Herzog and U. Osterwalder, Pure Appl. Chem. **87** (9-10), 937 (2015). <https://www.degruyter.com/view/j/pac.2015.87.issue-9-10/pac-2015-0401/pac-2015-0401.xml>.

[76] N. Serpone, D. Dondi, and A. Albini, Inorg. Chim. Acta **360** (3), 794 (2007). <http://www.sciencedirect.com/science/article/pii/S0020169306000259>, Protagonists in Chemistry: Vincenzo Balzani.

[77] C. Antoniou, M. G. Kosmadaki, A. J. Stratigos, and A. D. Katsambas, J. Eur. Acad. Dermatol. Venereol. **22** (9), 1110 (2008). <https://onlinelibrary.wiley.com/doi/abs/10.1111/j.1468-3083.2007.02580.x>.

[78] J. F. Nash and P. R. Tanner, Photodermatol. Photoimmunol. Photomed. **30** (2–3), 88 (2014). <https://onlinelibrary.wiley.com/doi/abs/10.1111/phpp.12113>.

[79] M. Schlumpf, S. Durrer, O. Faass, C. Ehnes, M. Fuetsch, C. Gaille, M. Henseler, L. Hofkamp, K. Maerkel, S. Reolon, B. Timms, J. A. F. Tresguerres, *et al.*, Int. J. Androl. **31** (2), 144 (2008). <https://onlinelibrary.wiley.com/doi/abs/10.1111/j.1365-2605.2007.00856.x>.

[80] S. Q. Wang, P. R. Tanner, H. W. Lim, and J. F. Nash, Photochem. Photobiol. Sci. **12**, 197 (2013). <http://dx.doi.org/10.1039/C2PP25112D>.

[81] S. Afonso, K. Horita, J. P. S. e Silva, I. F. Almeida, M. H. Amaral, P. A. Lobão, P. C. Costa, M. S. Miranda, J. C. G. E. da Silva, and J. M. S. Lobo, J. Photoch. Photobio. B **140**, 36 (2014). <http://www.sciencedirect.com/science/article/pii/S101113441400222X>.

[82] W. Schwack and T. Rudolph, J. Photoch. Photobio. B **28** (3), 229 (1995). <http://www.sciencedirect.com/science/article/pii/101113449507118L>.

[83] I. Karlsson, L. Hillerström, A. L. Stenfeldt, J. Mårtensson, and A. Börje, Chem. Res. Toxicol. **22** (11), 1881 (2009). <https://doi.org/10.1021/tx900284e>.

[84] N. A. Shaath, Photochem. Photobiol. Sci **9** (4), 464 (2010). <https://pubs.rsc.org/en/content/articlelanding/2010/pp/b9pp00174c>.

[85] V. Lhiaubet-Vallet, M. Marin, O. Jimenez, O. Gorchs, C. Trullas, and M. A. Miranda, Photochem. Photobiol. Sci. **9**, 552 (2010). <http://dx.doi.org/10.1039/B9PP00158A>.

[86] L. Gaspar and P. M. Campos, Int. J. Pharm. **307** (2), 123 (2006). <http://www.sciencedirect.com/science/article/pii/S0378517305006496>.

[87] A. Kikuchi, Y. Nakabai, N. Oguchi-Fujiyama, K. Miyazawa, and M. Yagi, J. Lumin. **166**, 203 (2015). <http://www.sciencedirect.com/science/article/pii/S002223131500280X>.

[88] R. M. Sayre, J. C. Dowdy, A. J. Gerwig, W. J. Shlelds, and R. V. Lioyd, Photochem. Photobiol. **81** (2), 452 (2005). <https://onlinelibrary.wiley.com/doi/abs/10.1111/j.1751-1097.2005.tb00207.x>.

[89] E. Chatelain and B. Gabard, Photochem. Photobiol. **74** (3), 401 (2001). <https://onlinelibrary.wiley.com/doi/abs/10.1562/0031-8655%282001%290740401POBMAA2.0.CO2>.

[90] J. A. Ruszkiewicz, A. Pinkas, B. Ferrer, T. V. Peres, A. Tsatsakis, and M. Aschner, Toxicol. Rep. **4**, 245 (2017). <http://www.sciencedirect.com/science/article/pii/S2214750017300288>.

[91] J. Wang, L. Pan, S. Wu, L. Lu, Y. Xu, Y. Zhu, M. Guo, and S. Zhuang, Int. J. Environ. Res. Public Health **13** (8), 782 (2016). <http://www.mdpi.com/1660-4601/13/8/782>.

[92] M. Krause, A. Klit, M. Blomberg Jensen, T. Søeborg, H. Frederiksen, M. Schlumpf, W. Lichtensteiger, N. E. Skakkebaek, and K. T. Drzewiecki, Int. J. Androl. **35** (3), 424 (2012). <https://onlinelibrary.wiley.com/doi/abs/10.1111/j.1365-2605.2012.01280.x>.

[93] M. S. Díaz-Cruz, M. Llorca, and D. Barceló, Trend. Anal. Chem **27** (10), 873 (2008).

[94] J. M. Brausch and G. M. Rand, Chemosphere **82** (11), 1518 (2011). <http://www.sciencedirect.com/science/article/pii/S0045653510013007>.

[95] C. B. Park, J. Jang, S. Kim, and Y. J. Kim, Ecotox. Environ. Safe. **137**, 57 (2017). <http://www.sciencedirect.com/science/article/pii/S0147651316304912>.

[96] R. Danovaro, L. Bongiorni, C. Corinaldesi, D. Giovannelli, E. Damiani, P. Astolfi, L. Greci, and A. Pusceddu, Environ. Health Persp. **116** (4), 441 (2008).

[97] R. B. Raffa, J. V. Pergolizzi Jr., R. Taylor Jr., and J. M. Kitzen, J. Clin. Pharm. Ther. **44** (1), 134 (2019). <https://onlinelibrary.wiley.com/doi/abs/10.1111/jcpt.12778>.

[98] C. A. Downs, E. Kramarsky-Winter, R. Segal, J. Fauth, S. Knutson, O. Bronstein, F. R. Ciner, R. Jeger, Y. Lichtenfeld, C. M. Woodley, P. Pennington, K. Cadenas, *et al.*, Arch. Environ. Con, Tox. **70** (2), 265 (2016). <https://doi.org/10.1007/s00244-015-0227-7>.

[99] D. Strickland and G. Mourou, Opt. Commun. **55** (6), 447 (1985). <https://doi.org/10.1016/0030-4018(85)90151-8>.

[100] J. Squier, F. Salin, G. Mourou, and D. Harter, Opt. Lett. **16** (5), 324 (1991). <http://0-ol.osa.org/abstract.cfm?URI=ol-16-5-324>.

[101] N. F. Scherer, J. L. Knee, D. D. Smith, and A. H. Zewail, J. Phys. Chem. **89** (24), 5141 (1985). <https://doi.org/10.1021/j100270a001>.

[102] A. H. Zewail, Science **242** (4886), 1645 (1988). <https://science.sciencemag.org/content/242/4886/1645>.

[103] A. H. Zewail, J. Phys. Chem. A **104** (24), 5660 (2000). <https://doi.org/10.1021/jp001460h>.

[104] A. H. Zewail, Angew. Chem. Int. Ed. **39** (15), 2586 (2000). <https://onlinelibrary.wiley.com/doi/abs/10.1002/1521-3773%2820000804%2939%3A15%3C2586%3A%3AAID-ANIE2586%3E3.0.CO%3B2-O>.

[105] V. G. Stavros and J. R. R. Verlet, Annu. Rev. Phys. Chem **67** (1), 211 (2016). <https://doi.org/10.1146/annurev-physchem-040215-112428>.

[106] H. H. Fielding and G. A. Worth, Chem. Soc. Rev. **47**, 309 (2018). <http://dx.doi.org/10.1039/C7CS00627F>.

[107] M. Staniforth and V. G. Stavros, Proc. R. Soc. A **469** (2159), 20130458 (2013). <https://royalsocietypublishing.org/doi/abs/10.1098/rspa.2013.0458>.

[108] A. Stolow, A. E. Bragg, and D. M. Neumark, Chem. Rev. **104** (4), 1719 (2004). <https://doi.org/10.1021/cr020683w>.

[109] B. Baguenard, J. B. Wills, F. Pagliarulo, F. Lépine, B. Climen, M. Barbaire, C. Clavier, M. A. Lebeault, and C. Bordas, Rev. Sci. Instrum. **75** (2), 324 (2004). <https://doi.org/10.1063/1.1642749>.

[110] I. V. Hertel and W. Radloff, Rep. Prog. Phys **69** (6), 1897 (2006). <https://doi.org/10.1088%2F0034-4885%2F69%2F6%2Fr06>.

[111] M. V. Johnston, Trend. Anal. Chem **3** (2), 58 (1984). <http://www.sciencedirect.com/science/article/pii/0165993684870557>.

[112] U. Even, J. Jortner, D. Noy, N. Lavie, and C. Cossart-Magos, J. Chem. Phys. **112** (18), 8068 (2000).

[113] D. Irimia, R. Kortekaas, and M. H. M. Janssen, Phys. Chem. Chem. Phys. **11**, 3958 (2009). <http://dx.doi.org/10.1039/B822960K>.

[114] D. Irimia, D. Dobrikov, R. Kortekaas, H. Voet, D. A. van den Ende, W. A. Groen, and M. H. M. Janssen, Rev. Sci. Instrum. **80** (11), 113303 (2009). <https://doi.org/10.1063/1.3263912>.

[115] C. Meng and M. H. M. Janssen, Rev. Sci. Instrum. **86** (2), 023110 (2015). <https://doi.org/10.1063/1.4913251>.

[116] W. C. Wiley and I. H. McLaren, Rev. Sci. Instrum. **26** (12), 1150 (1955). <https://doi.org/10.1063/1.1715212>.

[117] T. Streibel and R. Zimmermann, Annu. Rev. Anal. Chem **7** (1), 361 (2014). <https://doi.org/10.1146/annurev-anchem-062012-092648>.

[118] F. Gunzer, S. Krüger, and J. Grotemeyer, Mass Spectrom. Rev. **38** (2), 202 (2019). <https://onlinelibrary.wiley.com/doi/abs/10.1002/mas.21579>.

[119] N. d. N. Rodrigues, M. Staniforth, and V. G. Stavros, Proc. R. Soc. A **472** (2195), 20160677 (2016). <https://royalsocietypublishing.org/doi/full/10.1098/rspa.2016.0677>.

[120] S. Ullrich, T. Schultz, M. Z. Zgierski, and A. Stolow, Phys. Chem. Chem. Phys. **6**, 2796 (2004). <http://dx.doi.org/10.1039/B316324E>.

[121] S. H. Lee, K. C. Tang, I. C. Chen, M. Schmitt, J. P. Shaffer, T. Schultz, J. G. Underwood, M. Z. Zgierski, and A. Stolow, J. Phys. Chem. A **106** (39), 8979 (2002).

https://doi.org/10.1021/jp021096h>.

[122] D. R. Cyr and C. C. Hayden, J. Chem. Phys. **104** (2), 771 (1996). <https://doi.org/10.1063/1.470802>.

[123] A. W. Jasper, C. Zhu, S. Nangia, and D. G. Truhlar, Faraday Discuss. **127**, 1 (2004). <http://dx.doi.org/10.1039/B405601A>.

[124] A. Stolow, Int. Rev. Phys. Chem. **22** (2), 377 (2003). <https://doi.org/10.1080/0144235031000092448>.

[125] D. W. Chandler and P. L. Houston, J. Chem. Phys **87** (2), 14457 (1987). <https://doi.org/10.1063/1.453276>.

[126] A. T. J. B. Eppink and D. H. Parker, Rev. Sci. Instrum. **68** (9), 3477 (1997). <https://doi.org/10.1063/1.1148310>.

[127] C. Vallance, Phil. Trans. R. Soc. Lond. A **362** (1825), 2591 (2004). <https://royalsocietypublishing.org/doi/abs/10.1098/rsta.2004.1460>.

[128] M. N. R. Ashfold, N. H. Nahler, A. J. Orr-Ewing, O. P. J. Vieuxmaire, R. L. Toomes, T. N. Kitsopoulos, I. A. Garcia, D. A. Chestakov, S. M. Wu, and D. H. Parker, Phys. Chem. Chem. Phys. **8**, 26 (2006). <http://dx.doi.org/10.1039/B509304J>.

[129] A. I. Chichinin, K. H. Gericke, S. Kauczok, and C. Maul, Int. Rev. Phys. Chem **28** (4), 607 (2009). <https://doi.org/10.1080/01442350903235045>.

[130] S. J. Greaves, R. A. Rose, and A. J. Orr-Ewing, Phys. Chem. Chem. Phys. **12**, 9129 (2010). <http://dx.doi.org/10.1039/C001233E>.

[131] E. Szymańska, V. S. Prabhudesai, N. J. Mason, and E. Krishnakumar, Phys. Chem. Chem. Phys **15** (3), 998 (2013). <https://pubs.rsc.org/en/content/articlelanding/2012/cp/c2cp42966g>.

[132] C. J. Dasch, Appl. Opt. **31** (8), 1146 (1992). <http://ao.osa.org/abstract.cfm?URI=ao-31-8-1146>.

[133] G. M. Roberts, J. L. Nixon, J. Lecointre, E. Wrede, and J. R. R. Verlet, Rev. Sci. Instrum. **80** (5), 053104 (2009).

[134] N. d. N. Rodrigues, N. C. Cole-Filipiak, K. N. Blodgett, C. Abeysekera, T. S. Zwier, and V. G. Stavros, Nat. Commun. **9** (1), 5188 (2018). <https://www.nature.com/articles/s41467-018-07681-1>.

[135] S. Lochbrunner, T. Schultz, M. Schmitt, J. P. Shaffer, M. Z. Zgierski, and A. Stolow, J. Chem. Phys. **114** (6), 2519 (2001). <https://doi.org/10.1063/1.1345876>.

[136] B. Herzog, D. Hüglin, E. Borsos, A. Stehlin, and H. Luther, Chimia **58** (7–8), 554 (2004). <https://www.ingentaconnect.com/content/scs/chimia/2004/00000058/F0020007/art00002>.

[137] A. Stolow, Annu. Rev. Phys. Chem. **54** (1), 89 (2003). <https://www.annualreviews.org/doi/abs/10.1146/annurev.physchem.54.011002.103809>.

[138] G. Wu, P. Hockett, and A. Stolow, Phys. Chem. Chem. Phys. **13**, 18447 (2011). <http://dx.doi.org/10.1039/C1CP22031D>.

[139] T. Suzuki, Annu. Rev. Phys. Chem. **57** (1), 555 (2006). <https://doi.org/10.1146/annurev.physchem.57.032905.104601>.

[140] J. R. R. Verlet, Chem. Soc. Rev. **37**, 505 (2008). <http://dx.doi.org/10.1039/B700528H>.

[141] G. M. Roberts and V. G. Stavros, Chem. Sci. **5**, 1698 (2014). <http://dx.doi.org/10.1039/C3SC53175A>.

[142] J. C. Dean, R. Kusaka, P. S. Walsh, F. Allais, and T. S. Zwier, J. Am. Chem. Soc. **136** (42), 14780 (2014). <https://doi.org/10.1021/ja5059026>.

[143] D. Shimada, R. Kusaka, Y. Inokuchi, M. Ehara, and T. Ebata, Phys. Chem. Chem. Phys. **14**, 8999 (2012). <http://dx.doi.org/10.1039/C2CP24056D>.

[144] Y. Miyazaki, K. Yamamoto, J. Aoki, T. Ikeda, Y. Inokuchi, M. Ehara, and T. Ebata, J. Chem. Phys. **141** (24), 244313 (2014). <https://doi.org/10.1063/1.4904268>.

[145] K. Yamazaki, Y. Miyazaki, Y. Harabuchi, T. Taketsugu, S. Maeda, Y. Inokuchi, S. n. Kinoshita, M. Sumida, Y. Onitsuka, H. Kohguchi, M. Ehara, and T. Ebata, J. Phys. Chem. Lett. **7** (19), 4001 (2016). <https://doi.org/10.1021/acs.jpclett.6b01643>.

[146] S. n. Kinoshita, Y. Miyazaki, M. Sumida, Y. Onitsuka, H. Kohguchi, Y. Inokuchi, N. Akai, T. Shiraogawa, M. Ehara, K. Yamazaki, Y. Harabuchi, S. Maeda, *et al.*, Phys. Chem. Chem. Phys. **20**, 17583 (2018).

[147] S. n. Kinoshita, Y. Inokuchi, Y. Onitsuka, H. Kohguchi, N. Akai, T. Shiraogawa, M. Ehara, K. Yamazaki, Y. Harabuchi, S. Maeda, and T. Ebata, Phys. Chem. Chem. Phys. pp. – (2019). <http://dx.doi.org/10.1039/C9CP02914A>.

[148] S. Kenjo, Y. Iida, N. Chaki, S. n. Kinoshita, Y. Inokuchi, K. Yamazaki, and T. Ebata, Chem. Phys. **515**, 381 (2018). <http://www.sciencedirect.com/science/article/pii/S0301010418304208>.

[149] E. M. M. Tan, M. Hilbers, and W. J. Buma, J. Phys. Chem. Lett **5** (14), 2464 (2014). <https://pubs.acs.org/doi/abs/10.1021/jz501140b>.

[150] V. G. Stavros, Nat. Chem. **6** (11), 955 (2014). <https://www.nature.com/articles/nchem.2084>.

[151] S. R. Domingos and M. Schnell, J. Phys. Chem. Lett. **9** (17), 4963 (2018). <https://doi.org/10.1021/acs.jpclett.8b02029>.

[152] N. G. K. Wong, J. A. Berenbeim, M. Hawkridge, E. Matthews, and C. E. H. Dessent, Phys. Chem. Chem. Phys. **21**, 14311 (2019). <http://dx.doi.org/10.1039/C8CP06794E>.

[153] C. Ehlers, U. I. Ivens, M. L. Møller, T. Senderovitz, and J. Serup, Skin Res. Technol. **7** (2), 90 (2001). <https://onlinelibrary.wiley.com/doi/abs/10.1034/j.1600-0846.2001.70206.x>.

[154] K. M. S. Hansen, H. J. Albrechtsen, and H. R. Andersen, Journal of Water and Health **11** (3), 465 (2013). <https://dx.doi.org/10.2166/wh.2013.156>.

[155] L. A. Baker and V. G. Stavros, Sci. Prog. **99** (3), 282 (2016). <https://doi.org/10.3184/003685016X14684992086383>.

[156] A. Maciejewski, R. Naskrecki, M. Lorenc, M. Ziolek, J. Karolczak, J. Kubicki, M. Matysiak, and M. Szymanski, J. Mol. Struct. **555** (1), 1 (2000). <http://www.sciencedirect.com/science/article/pii/S0022286000005822>.

[157] R. Berera, R. van Grondelle, and J. T. M. Kennis, Photosynth. Res. **101** (2-3), 105 (2009). <https://link.springer.com/article/10.1007/s11120-009-9454-y>.

[158] C. Ruckebusch, M. Sliwa, P. Pernot, A. de Juan, and R. Tauler, J. Photoch. Photobio. C **13** (1), 1 (2012). <http://www.sciencedirect.com/science/article/pii/S1389556711000748>.

[159] L. A. Baker, B. Marchetti, T. N. V. Karsili, V. G. Stavros, and M. N. R. Ashfold, Chem. Soc. Rev. **46**, 3770 (2017). <http://dx.doi.org/10.1039/C7CS00102A>.

[160] I. H. van Stokkum, D. S. Larsen, and R. van Gron-

delle, Biochim. Biophys. Acta **1657** (2), 82 (2004). <http://www.sciencedirect.com/science/article/pii/S0005272804001094>.

[161] L. A. Baker, M. D. Horbury, S. E. Greenough, P. M. Coulter, T. N. V. Karsili, G. M. Roberts, A. J. Orr-Ewing, M. N. R. Ashfold, and V. G. Stavros, J. Phys. Chem. Lett. **6** (8), 1363 (2015).

[162] T. Steinel, J. B. Asbury, J. Zheng, and M. D. Fayer, J. Phys. Chem. A **108** (50), 10957 (2004). <https://doi.org/10.1021/jp046711r>.

[163] X. Tan, T. L. Gustafson, C. Lefumeux, G. Burdzinski, G. Buntinx, and O. Poizat, J. Phys. Chem. A **106** (14), 3593 (2002). <https://doi.org/10.1021/jp013176b>.

[164] S. Woutersen, U. Emmerichs, and H. J. Bakker, Science **278** (5338), 658 (1997). <http://science.sciencemag.org/content/278/5338/658>.

[165] M. Banno, K. Ohta, S. Yamaguchi, S. Hirai, and K. Tominaga, Acc. Chem. Res. **42** (9), 1259 (2009). <https://doi.org/10.1021/ar9000229>.

[166] C. Manzoni, D. Polli, and G. Cerullo, Rev. Sci. Instrum. **77** (2), 023103 (2006). <https://doi.org/10.1063/1.2167128>.

[167] A. C. Cozzi, P. Perugini, and S. Gourion-Arsiquaud, Eur. J. Pharm. Sci **121**, 309 (2018). <http://www.sciencedirect.com/science/article/pii/S0928098718302574>.

[168] M. Han, D. Ishikawa, E. Muto, and M. Hara, J. Lumin. **129** (10), 1163 (2009). <http://www.sciencedirect.com/science/article/pii/S0022231309003032>.

[169] N. S. Bora, B. Mazumder, and P. Chattopadhyay, J. Dermatol. Treat. **29** (3), 256 (2018). <https://doi.org/10.1080/09546634.2017.1364691>, PMID: 28783990.

[170] F. H. Yap, H. C. Chua, and C. P. Tait, Australas. J. Dermatol. **58** (4), e160 (2017). <https://onlinelibrary.wiley.com/doi/abs/10.1111/ajd.12597>.

[171] N. d. N. Rodrigues, N. C. Cole-Filipiak, M. D. Horbury, M. Staniforth, T. N. V. Karsili, Y. Peperstraete, and V. G. Stavros, J. Photoch. Photobio. A **353**, 376 (2018). <http://www.sciencedirect.com/science/article/pii/S101060301731434X>.

[172] L. E. Agrapidis-Paloympis, R. A. Nash, and N. A. Shaath, J. Soc. Cosmet. Chem. **38**, 209 (1987).

[173] A. Beeby and A. E. Jones, Photochem. Photobiol. **72** (1), 10 (2000). <https://doi.org/10.1562/0031-8655(2000)0720010TPPOMA2.0.CO2>.

[174] A. Kikuchi, K. Shibata, R. Kumasaka, and M. Yagi, Photochem. Photobiol. Sci. **12**, 246 (2013). <http://dx.doi.org/10.1039/C2PP25190F>.

[175] B. Poljšak and R. Dahmane, Dermatol. Res. Pract. **2012**, 135206 (2012). <https://www.hindawi.com/journals/drp/2012/135206/cta/>.

[176] S. Matsumoto, R. Kumasaka, M. Yagi, and A. Kikuchi, J. Photoch. Photobio. A **346**, 396 (2017). <http://www.sciencedirect.com/science/article/pii/S1010603017304872>.

[177] J. S. Mulliken, J. E. Russak, and D. S. Rigel, Dermatol. Clin. **30** (3), 369 (2012). <http://www.sciencedirect.com/science/article/pii/S0733863512000344>.

[178] D. R. Yarkony, Rev. Mod. Phys. **68**, 985 (1996). <https://link.aps.org/doi/10.1103/RevModPhys.68.985>.

[179] D. R. Yarkony, Acc. Chem. Res. **31** (8), 511 (1998). <https://doi.org/10.1021/ar970113w>.

[180] F. Bernardi, M. Olivucci, and M. A. Robb, Chem. Soc. Rev. **25**, 321 (1996). <http://dx.doi.org/10.1039/CS9962500321>.

[181] S. Matsika and P. Krause, Annu. Rev. Phys. Chem. **62** (1), 621 (2011). <https://doi.org/10.1146/annurev-physchem-032210-103450>.

[182] W. Fuß, S. Lochbrunner, A. Müller, T. Schikarski, W. Schmid, and S. Trushin, Chem. Phys. **232** (1), 161 (1998). <http://www.sciencedirect.com/science/article/pii/S0301010498001141>.

[183] G. A. Worth and L. S. Cederbaum, Annu. Rev. Phys. Chem. **55** (1), 127 (2004). <https://doi.org/10.1146/annurev.physchem.55.091602.094335>.

[184] A. L. Sobolewski and W. Domcke, Europhys. News **37** (4), 20 (2006). <http://dx.doi.org/10.1051/epn:2006405>.

[185] A. H. Zewail, J. Phys. Chem. **97** (48), 12427 (1993). <https://doi.org/10.1021/j100150a001>.

[186] M. Józefowicz, J. R. Heldt, and J. Heldt, J. Lumin. **132** (3), 755 (2012). <http://www.sciencedirect.com/science/article/pii/S0022231311005990>.

[187] P. Hepworth, J. McCombie, J. Simons, J. Pfanstiel, J. Ribblett, and D. Pratt, Chem. Phys. Lett. **249** (5), 341 (1996). <http://www.sciencedirect.com/science/article/pii/0009261495013814>.

[188] N. d. N. Rodrigues, N. C. Cole-Filipiak, M. A. P. Turner, K. Krokidi, G. L. Thornton, G. W. Richings, N. D. M. Hine, and V. G. Stavros, Chem. Phys. **515**, 596 (2018). <http://www.sciencedirect.com/science/article/pii/S0301010418305937>.

[189] M. Promkatkaew, S. Suramitr, T. Karpkird, S. Wanichwecharungruang, M. Ehara, and S. Hannongbua, Photochem. Photobiol. Sci. **13** (3), 583 (2014). <https://pubs.rsc.org/en/content/articlelanding/2014/pp/c3pp50319d>.

[190] W. H. Melhuish, J. Phys. Chem. **65** (2), 229 (1961). <https://doi.org/10.1021/j100820a009>.

[191] O. P. J. Vieuxmaire, Z. Lan, A. L. Sobolewski, and W. Domcke, J. Chem. Phys. **129** (22), 224307 (2008). <https://doi.org/10.1063/1.3028049>.

[192] B. Lasorne, M. J. Bearpark, M. A. Robb, and G. A. Worth, J. Phys. Chem. A **112** (50), 13017 (2008). <https://doi.org/10.1021/jp803740a>.

[193] L. Blancafort and M. A. Robb, J. Chem. Theory Comput. **8** (12), 4922 (2012). <https://doi.org/10.1021/ct300625u>.

[194] I. J. Palmer, I. N. Ragazos, F. Bernardi, M. Olivucci, and M. A. Robb, J. Am. Chem. Soc. **115** (2), 673–682 (1993). <https://doi.org/10.1021/ja00055a042>.

[195] A. D. Dunkelberger, R. D. Kieda, B. M. Marsh, and F. Fleming Crim, J. Phys. Chem. A **119** (24), 6155 (2015). <https://pubs.acs.org/doi/abs/10.1021/acs.jpca.5b01641>.

[196] L. A. Baker, S. L. Clark, S. Habershon, and V. G. Stavros, J. Phys. Chem. Lett. **8** (10), 2113 (2017). <https://doi.org/10.1021/acs.jpclett.7b00633>.

[197] Y. Peperstraete, M. Staniforth, L. A. Baker, N. D. N. Rodrigues, N. C. Cole-Filipiak, W. D. Quan, and V. G. Stavros, Phys. Chem. Chem. Phys. **18**, 28140 (2016). <http://dx.doi.org/10.1039/C6CP05205C>.

[198] L. A. Baker, M. D. Horbury, and V. G. Stavros, Opt. Express **24** (10), 10700 (2016). <http://www.opticsexpress.org/abstract.cfm?URI=oe-24-10-10700>.

[199] C. Ma, C. T. L. Chan, R. C. T. Chan, A. K. W. Wong, B. P. Y. Chung, and W. M. Kwok, Phys. Chem. Chem. Phys. **20**, 24796 (2018). <http://dx.doi.org/10.1039/C8CP04447C>.

[200] L. A. Baker, M. D. Horbury, S. E. Greenough, M. N. R. Ash-

fold, and V. G. Stavros, Photochem. Photobiol. Sci. **14**, 1814 (2015). <http://dx.doi.org/10.1039/C5PP00217F>.

[201] M. T. Ignasiak, C. Houée-Levin, G. Kciuk, B. Marciniak, and T. Pedzinski, ChemPhysChem **16** (3), 628 (2015). <https://onlinelibrary.wiley.com/doi/abs/10.1002/cphc.201402703>.

[202] T. N. V. Karsili, B. Marchetti, M. N. R. Ashfold, and W. Domcke, J. Phys. Chem. A **118** (51), 11999 (2014). <https://doi.org/10.1021/jp507282d>.

[203] L. A. Baker, S. E. Greenough, and V. G. Stavros, J. Phys. Chem. Lett. **7** (22), 4655 (2016). <https://doi.org/10.1021/acs.jpclett.6b02104>, PMID: 27791379.

[204] C. X. Li, W. W. Guo, B. B. Xie, and G. Cui, J. Chem. Phys **145** (7), 074308 (2016). <https://doi.org/10.1063/1.4961261>.

[205] S. L. Schneider and H. W. Lim, Photodermatol. Photoimmunol. Photomed. p. 1 (2018). <https://onlinelibrary.wiley.com/doi/full/10.1111/phpp.12439>.

[206] L. A. Baker, L. C. Grosvenor, M. N. R. Ashfold, and V. G. Stavros, Chem. Phys. Lett. **664**, 39 (2016). <http://www.sciencedirect.com/science/article/pii/S0009261416307710>.

[207] S. L. Schneider and H. W. Lim, J. Am. Acad. Dermatol. **80** (1), 266 (2019). <https://doi.org/10.1016/j.jaad.2018.06.033>.

[208] J. C. DiNardo and C. A. Downs, J. Cosmet. Dermatol. **17** (1), 15 (2018). <https://onlinelibrary.wiley.com/doi/abs/10.1111/jocd.12449>.

[209] E. Gilbert, F. Pirot, V. Bertholle, L. Roussel, F. Falson, and K. Padois, Int. J. Cosmet. Sci. **35** (3), 208 (2013). <https://onlinelibrary.wiley.com/doi/abs/10.1111/ics.12030>.

[210] S. P. Huong, V. Andrieu, J. P. Reynier, E. Rocher, and J. D. Fourneron, J. Photoch. Photobio. A **186** (1), 65 (2007). <http://www.sciencedirect.com/science/article/pii/S101060300600400X>.

[211] A. Sharma, K. Bányiová, P. Babica, N. E. Yamani, A. R. Collins, and P. Čupr, Sci. Total Environ. **593-594**, 18 (2017). <http://www.sciencedirect.com/science/article/pii/S0048969717305478>.

[212] A. Sharma, K. Řiháčková, and P. Čupr, Sci. Total Environ. **657**, 902 (2019). <http://www.sciencedirect.com/science/article/pii/S0048969718348848>.

[213] K. M. Hanson, S. Narayanan, V. M. Nichols, and C. J. Bardeen, Photochem. Photobiol. Sci. **14**, 1607 (2015). <http://dx.doi.org/10.1039/C5PP00074B>.

[214] J. M. Woolley, J. S. Peters, M. A. P. Turner, G. J. Clarkson, M. D. Horbury, and V. G. Stavros, Phys. Chem. Chem. Phys. **21**, 14350 (2019). <http://dx.doi.org/10.1039/C8CP06536E>.

[215] Y. Miyazaki, Y. Inokuchi, N. Akai, and T. Ebata, J. Phys. Chem. Lett. **6** (7), 1134 (2015). <https://doi.org/10.1021/acs.jpclett.5b00203>.

[216] P. Morlière, O. Avice, T. S. E. Melo, L. Dubertret, M. Giraud, and R. Santus, Photochem. Photobiol. **36** (4), 395 (1982). <https://onlinelibrary.wiley.com/doi/abs/10.1111/j.1751-1097.1982.tb04392.x>.

[217] M. Schlumpf, B. Cotton, M. Conscience, V. Haller, B. Steinmann, and W. Lichtensteiger, Environ. Health Persp. **109** (3), 239 (2001). <https://ehp.niehs.nih.gov/doi/abs/10.1289/ehp.01109239>.

[218] X. He, A. F. Bell, and P. J. Tonge, Org. Lett. **4** (9), 1523 (2002).

https://doi.org/10.1021/ol0200403>.

[219] T. M. Karpkird, S. Wanichweacharungruang, and B. Albinsson, Photochem. Photobiol. Sci. **8**, 1455 (2009). <http://dx.doi.org/10.1039/B909695G>.

[220] N. D. N. Rodrigues, M. Staniforth, J. D. Young, Y. Peperstraete, N. C. Cole-Filipiak, J. R. Gord, P. S. Walsh, D. M. Hewett, T. S. Zwier, and V. G. Stavros, Faraday Discuss. **194**, 709 (2016). <http://dx.doi.org/10.1039/C6FD00079G>.

[221] X. P. Chang, C. X. Li, B. B. Xie, and G. Cui, J. Phys. Chem. A **119** (47), 11488 (2015). <https://doi.org/10.1021/acs.jpca.5b08434>.

[222] K. Morabito, N. C. Shapley, K. G. Steeley, and A. Tripathi, Int. J. Cosmet. Sci. **33** (5), 385 (2011). <https://onlinelibrary.wiley.com/doi/abs/10.1111/j.1468-2494.2011.00654.x>.

[223] N. Saewan and A. Jimtaisong, J. Cosmet. Dermatol. **14** (1), 47 (2015). <https://onlinelibrary.wiley.com/doi/abs/10.1111/jocd.12123>.

[224] B. W. Shirley, Trends Plant Sci. **1** (11), 377 (1996). <http://www.sciencedirect.com/science/article/pii/S1360138596803128>.

[225] M. Brenner and V. J. Hearing, Photochem. Photobiol. **84** (3), 539 (2008). <https://onlinelibrary.wiley.com/doi/abs/10.1111/j.1751-1097.2007.00226.x>.

[226] J. P. Ortonne, Brit. J. Dermatol. **146**, 7 (2002). <https://doi.org/10.1046/j.1365-2133.146.s61.3.x>.

[227] Y. Liu, X. Zhao, J. Luo, and S. Yang, J. Lumin. **206**, 469 (2019). <http://www.sciencedirect.com/science/article/pii/S0022231318309943>.

[228] O. Hendrawati, Q. Yao, H. K. Kim, H. J. Linthorst, C. Erkelens, A. W. Lefeber, Y. H. Choi, and R. Verpoorte, Plant Sci. **170** (6), 1118 (2006). <http://www.sciencedirect.com/science/article/pii/S0168945206000343>.

[229] L. A. Baker, M. D. Horbury, S. E. Greenough, F. Allais, P. S. Walsh, S. Habershon, and V. G. Stavros, J. Phys. Chem. Lett. **7** (1), 56 (2016). <https://doi.org/10.1021/acs.jpclett.5b02474>.

[230] M. D. Horbury, W. D. Quan, A. L. Flourat, F. Allais, and V. G. Stavros, Phys. Chem. Chem. Phys. **19**, 21127 (2017). <http://dx.doi.org/10.1039/C7CP04070A>.

[231] X. Zhao, J. Luo, S. Yang, and K. Han, J. Phys. Chem. Lett. **10**, 4197 (2019). <https://doi.org/10.1021/acs.jpclett.9b01651>.

[232] R. Haywood, P. Wardman, R. Sanders, and C. Linge, J. Invest. Dermatol. **121** (4), 862 (2003). <http://www.sciencedirect.com/science/article/pii/S0022202X15304437>.

[233] J. Snellenburg, S. Laptenok, R. Seger, K. Mullen, and I. Van Stokkum, J. Stat. Soft. **49** (3), 1 (2012). <https://hal-polytechnique.archives-ouvertes.fr/hal-00817159/>.

[234] K. M. Mullen and I. H. M. Van Stokkum, J. Stat. Soft **18** (3), 1 (2007). <http://dare.ubvu.vu.nl/bitstream/handle/1871/39958/225711.pdf?sequence=1>.

[235] L. A. Baker, M. Staniforth, A. L. Flourat, F. Allais, and V. G. Stavros, ChemPhotoChem **2** (8), 743 (2018). <https://onlinelibrary.wiley.com/doi/abs/10.1002/cptc.201800060>.

[236] J. Luo, Y. Liu, S. Yang, A. L. Flourat, F. Allais, and K. Han, J. Phys. Chem. Lett. **8** (5), 1025 (2017). <https://doi.org/10.1021/acs.jpclett.7b00083>.

[237] M. D. Horbury, L. A. Baker, N. D. Rodrigues, W. D. Quan, and V. G. Stavros, Chem. Phys. Lett. **673**, 62 (2017). <http://www.sciencedirect.com/science/article/pii/S0009261417301112>.

[238] M. D. Horbury, A. L. Flourat, S. E. Greenough, F. Allais, and V. G. Stavros, Chem. Commun. **54**, 936 (2018). <http://dx.doi.org/10.1039/C7CC09061G>.

[239] S. Jiang, S. Liu, and W. Feng, J. Mech. Behav. Biomed. **4** (7), 1228 (2011). <http://www.sciencedirect.com/science/article/pii/S1751616111000786>.

[240] E. A. Kamoun, E. R. S. Kenawy, and X. Chen, J. Adv. Res. **8** (3), 217 (2017). <http://www.sciencedirect.com/science/article/pii/S2090123217300243>.

[241] M. Morales-Hurtado, X. Zeng, P. Gonzalez-Rodriguez, J. T. Elshof, and E. van der Heide, J. Mech. Behav. Biomed. **46**, 305 (2015). <http://www.sciencedirect.com/science/article/pii/S1751616115000570>.

[242] C. Roullier, M. Chollet-Krugler, E. M. Pferschy-Wenzig, A. Maillard, G. N. Rechberger, B. Legouin-Gargadennec, R. Bauer, and J. Boustie, Phytochemistry **72** (11), 1348 (2011). <http://www.sciencedirect.com/science/article/pii/S0031942211002020>.

[243] W. M. Bandaranayake, Nat. Prod. Rep. **15**, 159 (1998). <http://dx.doi.org/10.1039/A815159Y>.

[244] S. Bhatia, A. Garg, K. Sharma, S. Kumar, A. Sharma, and A. Purohit, Pharmacogn. Rev. **5** (10), 138 (2011). <https://www.ncbi.nlm.nih.gov/pmc/articles/PMC3263047/>.

[245] T. Řezanka, M. Temina, A. G. Tolstikov, and V. M. Dembitsky, Folia Microbiol. **49** (4), 339 (2004). <https://doi.org/10.1007/BF03354663>.

[246] U. Karsten, T. Sawal, H. Dieter, K. Bischof, F. L. Figueroa, A. Flores-Moya, and C. Wiencke, Bot. Mar. **41**, 443 (1998). <https://doi.org/10.1515/botm.1998.41.1-6.443>.

[247] E. P. Balskus and C. T. Walsh, Science **329** (5999), 1653 (2010). <http://science.sciencemag.org/content/329/5999/1653>.

[248] R. P. Sinha, S. P. Singh, and D. P. Häder, J. Photoch. Photobio. B **89** (1), 29 (2007). <https://www.sciencedirect.com/science/article/pii/S101113440700108X>.

[249] D. Karentz, F. S. McEuen, M. C. Land, and W. C. Dunlap, Mar. Biol. **108** (1), 157 (1991). <https://doi.org/10.1007/BF01313484>.

[250] Q. Gao and F. Garcia-Pichel, Nat. Rev. Microbiol. **9** (11), 791 (2011). <https://www.nature.com/articles/nrmicro2649>.

[251] J. M. Shick and W. C. Dunlap, Annu. Rev. Physiol. **64** (1), 223 (2002). <https://doi.org/10.1146/annurev.physiol.64.081501.155802>.

[252] A. Oren and N. Gunde-Cimerman, FEMS Microbiol. Lett. **269** (1), 1 (2007). <https://doi.org/10.1111/j.1574-6968.2007.00650.x>.

[253] E. Chrapusta, A. Kaminski, K. Duchnik, B. Bober, M. Adamski, and J. Bialczyk, Mar. Drugs **15** (10), 326 (2017). <http://www.mdpi.com/1660-3397/15/10/326>.

[254] R. Losantos, I. Funes-Ardoiz, J. Aguilera, E. Herrera-Ceballos, C. García-Iriepa, P. J. Campos, and D. Sampedro, Angew. Chem. Int. Edit. **56** (10), 2632 (2017). <https://onlinelibrary.wiley.com/doi/abs/10.1002/anie.201611627>.

[255] D. Sampedro, Phys. Chem. Chem. Phys. **13**, 5584 (2011). <http://dx.doi.org/10.1039/C0CP02901G>.

[256] R. Losantos, M. S. Churio, and D. Sampedro, ChemistryOpen **4** (2), 155 (2015). <https://onlinelibrary.wiley.com/doi/abs/10.1002/open.201402125>.

[257] R. Losantos, D. Sampedro, and M. S. Churio, Pure Appl. Chem. **87** (9-10),

979 (2015). <https://www.degruyter.com/view/j/pac.2015.87.issue-9-10/pac-2015-0304/pac-2015-0304.xml>.

[258] R. Losantos, I. Lamas, R. Montero, A. Longarte, and D. Sampedro, Phys. Chem. Chem. Phys. **21**, 11376 (2019). <http://dx.doi.org/10.1039/C9CP01267B>.

[259] J. M. Woolley, M. Staniforth, M. D. Horbury, G. W. Richings, M. Wills, and V. G. Stavros, J. Phys. Chem. Lett. **9** (11), 3043 (2018). <https://doi.org/10.1021/acs.jpclett.8b00921>.

[260] B. Dietzek, T. Pascher, V. Sundström, and A. Yartsev, Laser Phys. Lett. **4** (1), 38 (2007). <https://doi.org/10.1002%2Flapl.200610070>.

[261] M. Lorenc, M. Ziolek, R. Naskrecki, J. Karolczak, J. Kubicki, and A. Maciejewski, Appl. Phys. B **74** (1), 19 (2002). <https://doi.org/10.1007/s003400100750>.

[262] X. X. Sui, L. Li, Y. Zhao, H. G. Wang, K. M. Pei, and X. Zheng, Spectrochim. Acta A **85** (1), 165 (2012). <http://www.sciencedirect.com/science/article/pii/S1386142511008699>.

[263] E. M. Arbeloa, S. G. Bertolotti, and M. S. Churio, Photochem. Photobiol. Sci. **10**, 133 (2011). <http://dx.doi.org/10.1039/C0PP00250J>.

[264] J. Kockler, M. Oelgemöller, S. Robertson, and B. D. Glass, Cosmetics **1** (2), 128 (2014). <https://www.mdpi.com/2079-9284/1/2/128>.

[265] E. Gregoris, S. Fabris, M. Bertelle, L. Grassato, and R. Stevanato, Int. J. Pharm. **405** (1), 97 (2011). <http://www.sciencedirect.com/science/article/pii/S0378517310009014>.

[266] G. Agati and M. Tattini, New Phytol. **186** (4), 786 (2010). <https://nph.onlinelibrary.wiley.com/doi/abs/10.1111/j.1469-8137.2010.03269.x>.

[267] H. Masaki, J. Dermatol. Sci. **58** (2), 85 (2010). <http://www.sciencedirect.com/science/article/pii/S0923181110000782>.

[268] S. Singer, S. Karrer, and M. Berneburg, Curr. Opin. Pharmacol. **46**, 24 (2019). <http://www.sciencedirect.com/science/article/pii/S1471489218301243>.

[269] B. H. Mahmoud, C. L. Hexsel, I. H. Hamzavi, and H. W. Lim, Photohem. Photobiol. **84** (2), 450 (2008). <https://onlinelibrary.wiley.com/doi/abs/10.1111/j.1751-1097.2007.00286.x>.

[270] J. Liebmann, M. Born, and V. Kolb-Bachofen, J. Invest. Dermatol. **130** (1), 259 (2010). <http://www.sciencedirect.com/science/article/pii/S0022202X1534519X>.

[271] M. M. Kleinpenning, T. Smits, M. H. A. Frunt, P. E. J. Van Erp, P. C. M. Van De Kerkhof, and R. M. J. P. Gerritsen, Photodermatol. Photoimmunol. Photomed. **26** (1), 16 (2010). <https://onlinelibrary.wiley.com/doi/abs/10.1111/j.1600-0781.2009.00474.x>.

[272] K. P. Lawrence, T. Douki, R. P. Sarkany, S. Acker, B. Herzog, and A. R. Young, Sci. Rep. **8**, 12772 (2018). <https://www.nature.com/articles/s41598-018-30738-6>.